Electronic Supplementary Material (ESI) for RSC Advances.

Supporting Information

Zr(IV) complexes containing salan-type ligands: Synthesis, structural characterization and role as catalysts towards the polymerization of ε-caprolactone, *rac*-lactide, ethylene, homopolymerization and copolymerization of epoxides with CO_2

Mrinmay Mandal,[a] Debashis Chakraborty*[a] and Venkatachalam Ramkumar[b]

[a]Department of Chemistry, Indian Institute of Technology Patna, Patna-800 013, Bihar, India. Tel: +91 6122552171. E-mail address: dc@iitp.ac.in; debashis.iitp@gmail.com (D. Chakraborty).

[b]Department of Chemistry, Indian Institute of Technology Madras, Chennai 600036, Tamil Nadu, India.

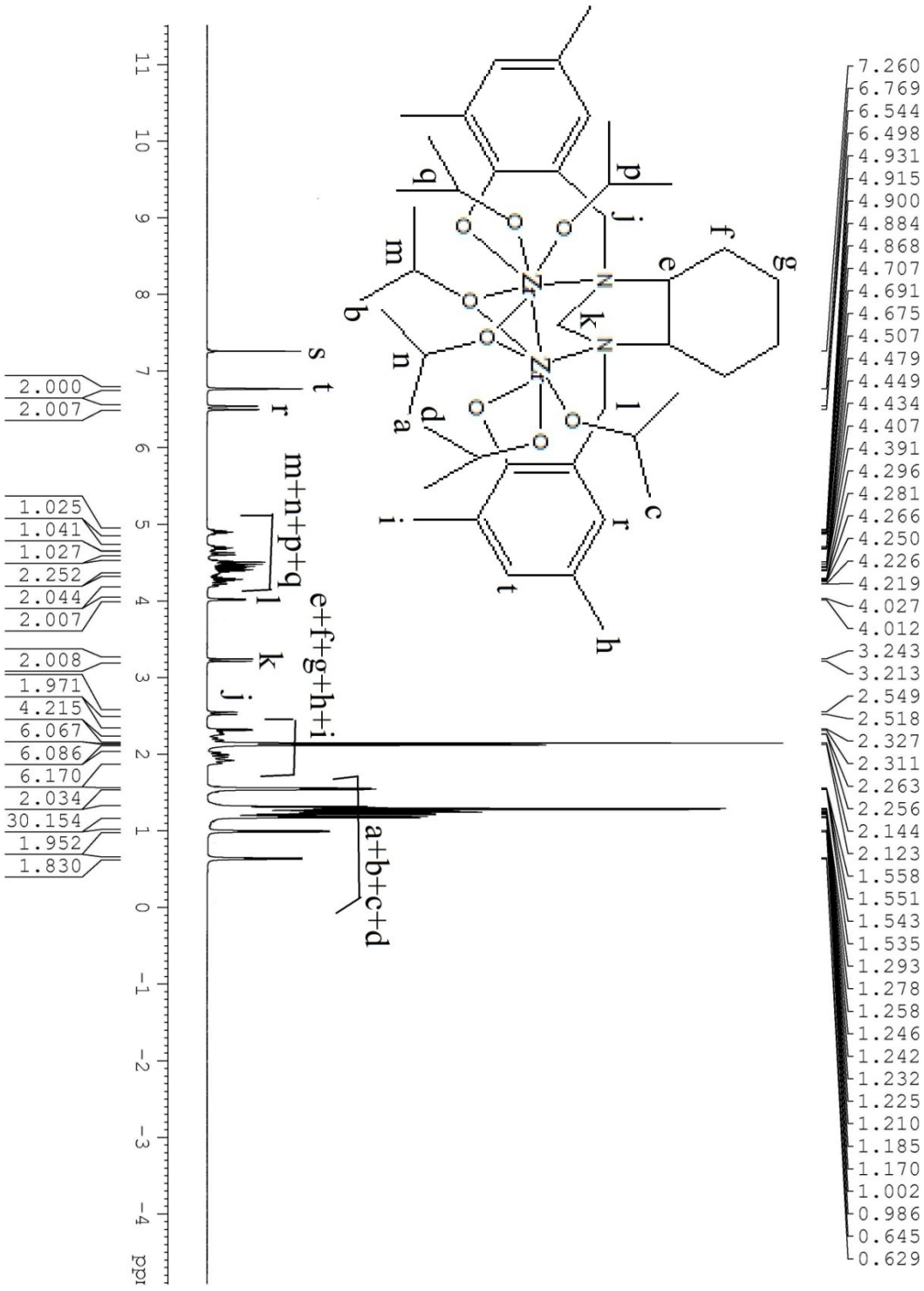

Fig. S1 ^{1}H NMR (400 MHz, $CDCl_3$) of Compound **1**

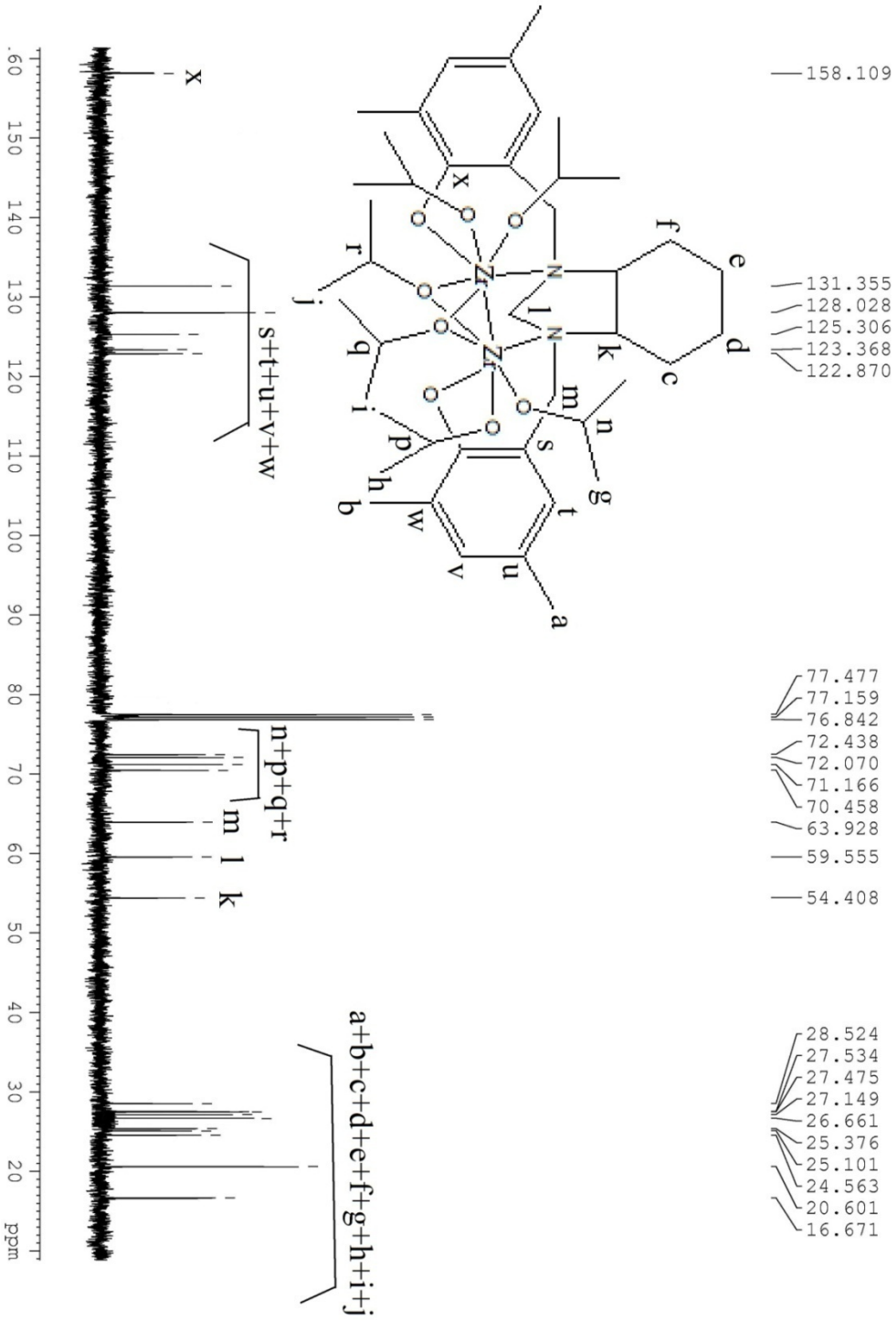

Fig. S2 ^{13}C NMR (100 MHz, $CDCl_3$) of Compound **1**

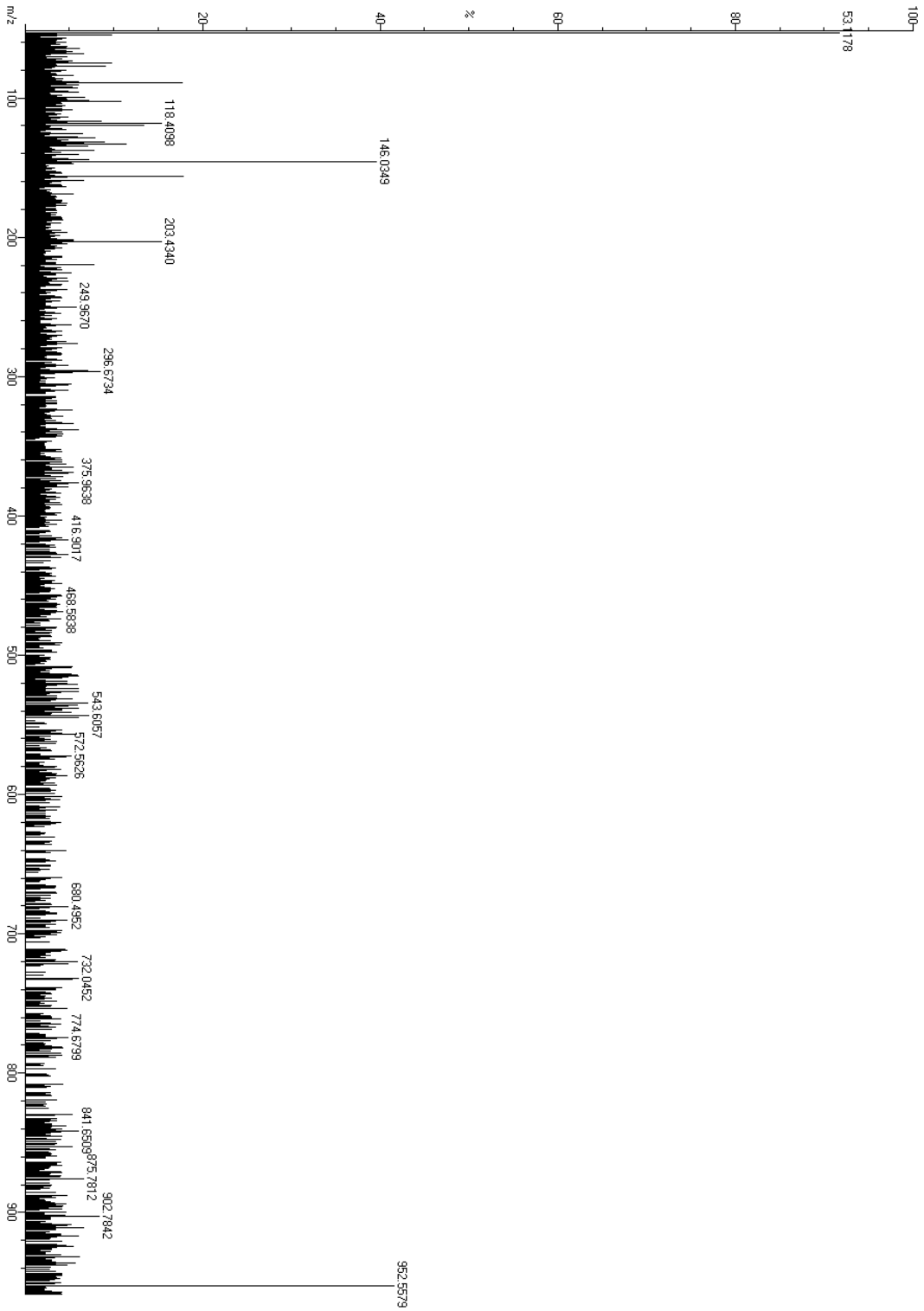

Fig. S3 ESI-Mass Spectrum of Compound **1**

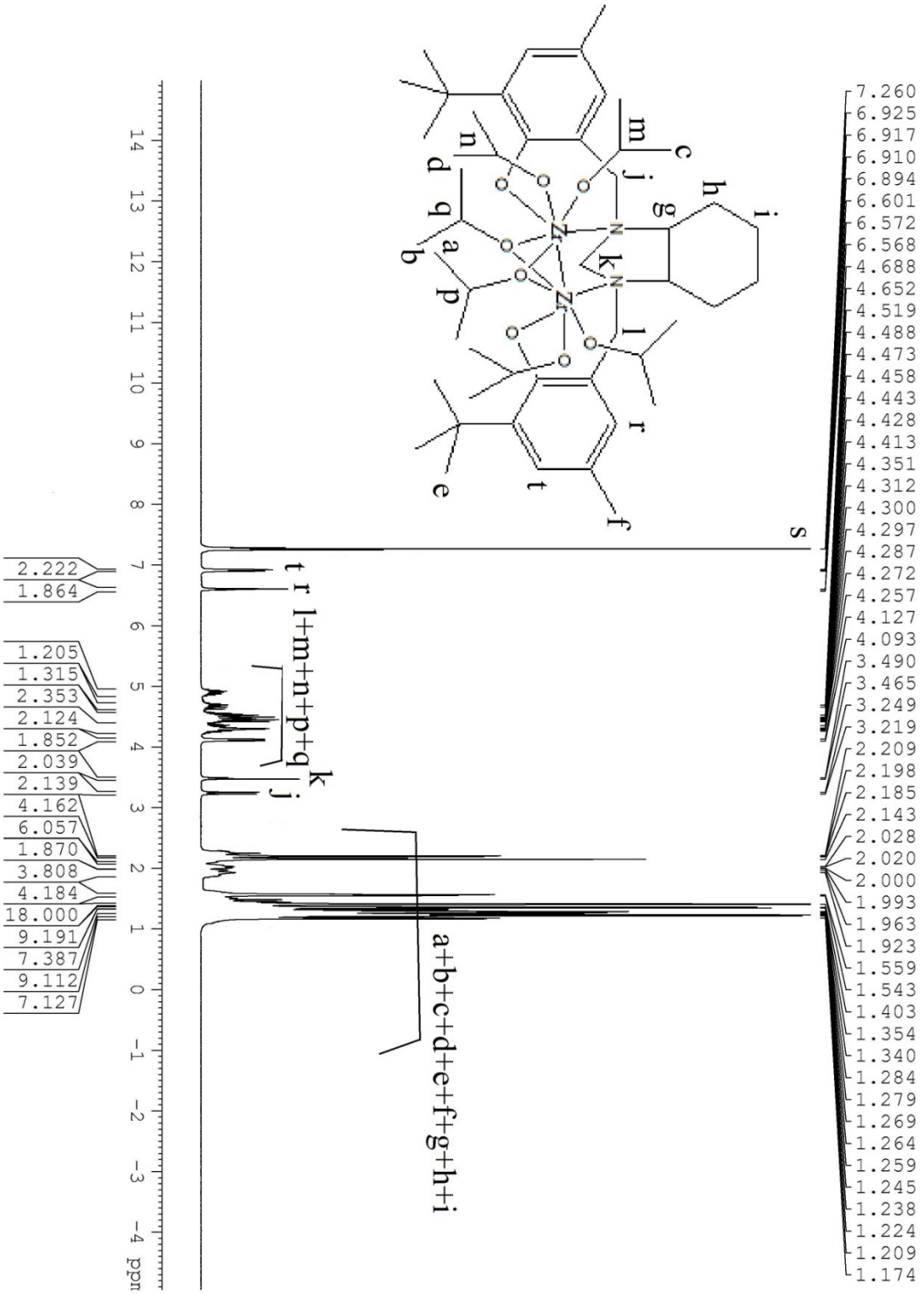

Fig. S4 ^{1}H NMR (400 MHz, $CDCl_3$) of Compound **2**

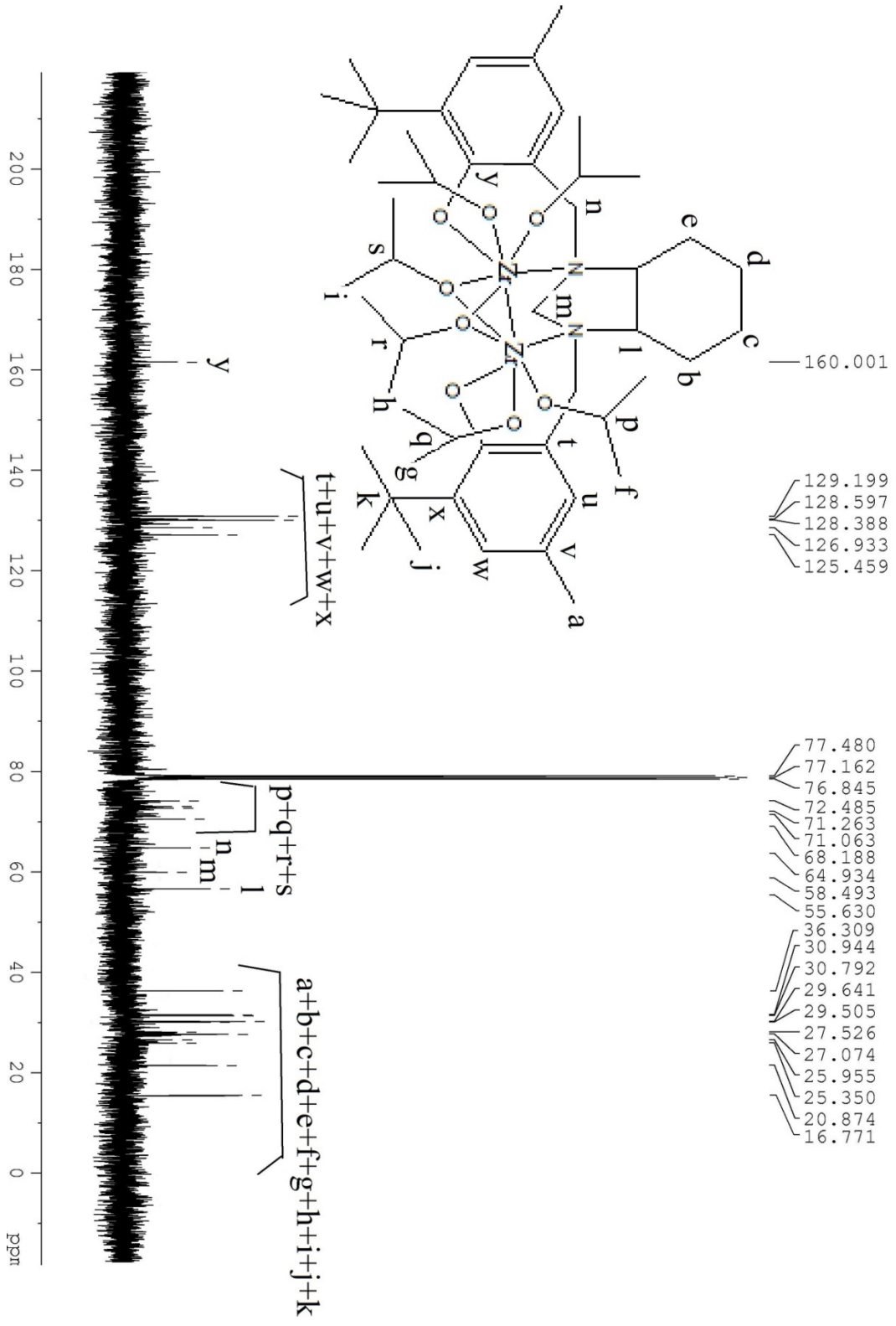

Fig. S5 ^{13}C NMR (100 MHz, $CDCl_3$) of Compound **2**

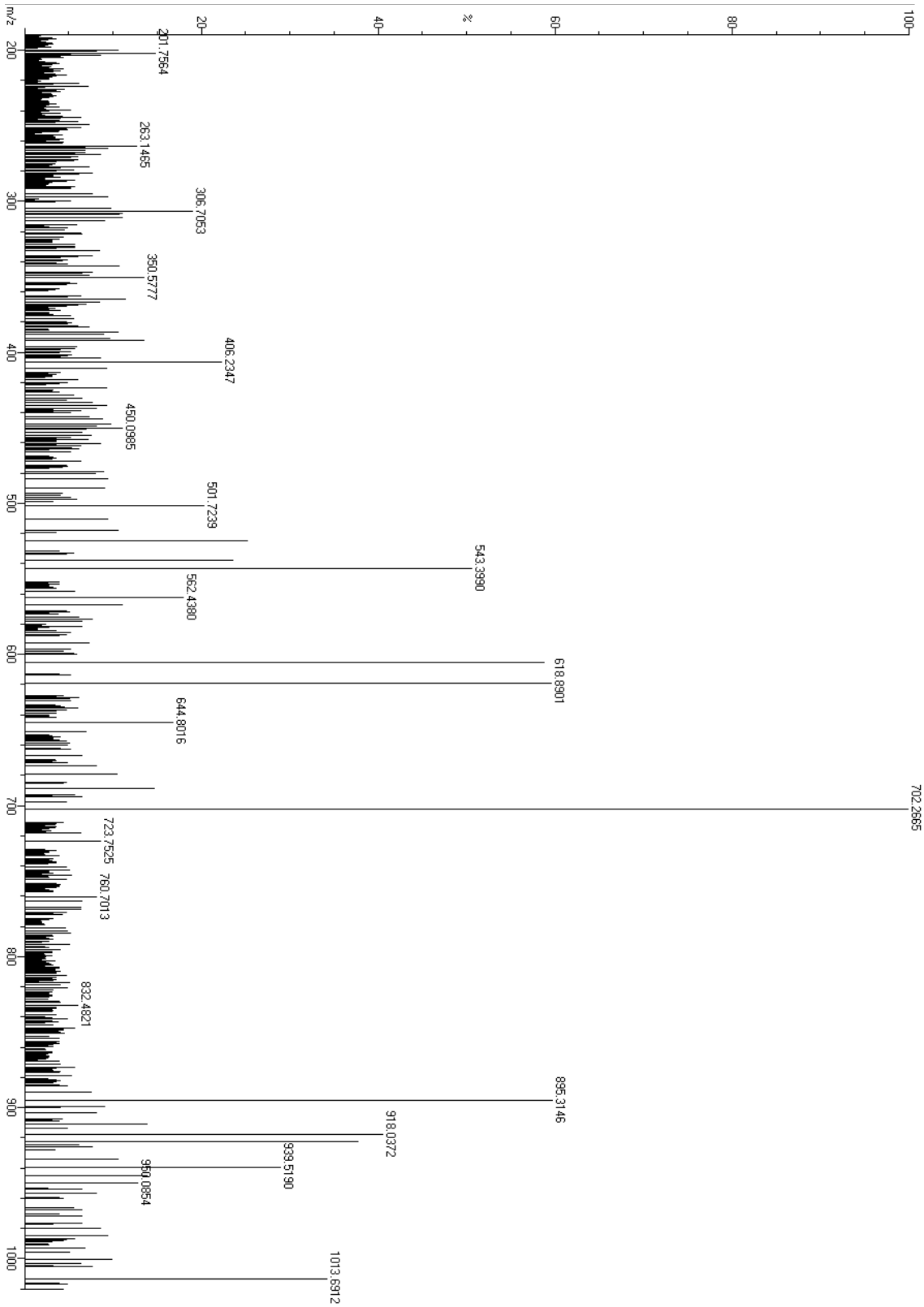

Fig. S6 ESI-Mass Spectrum of Compound **2**

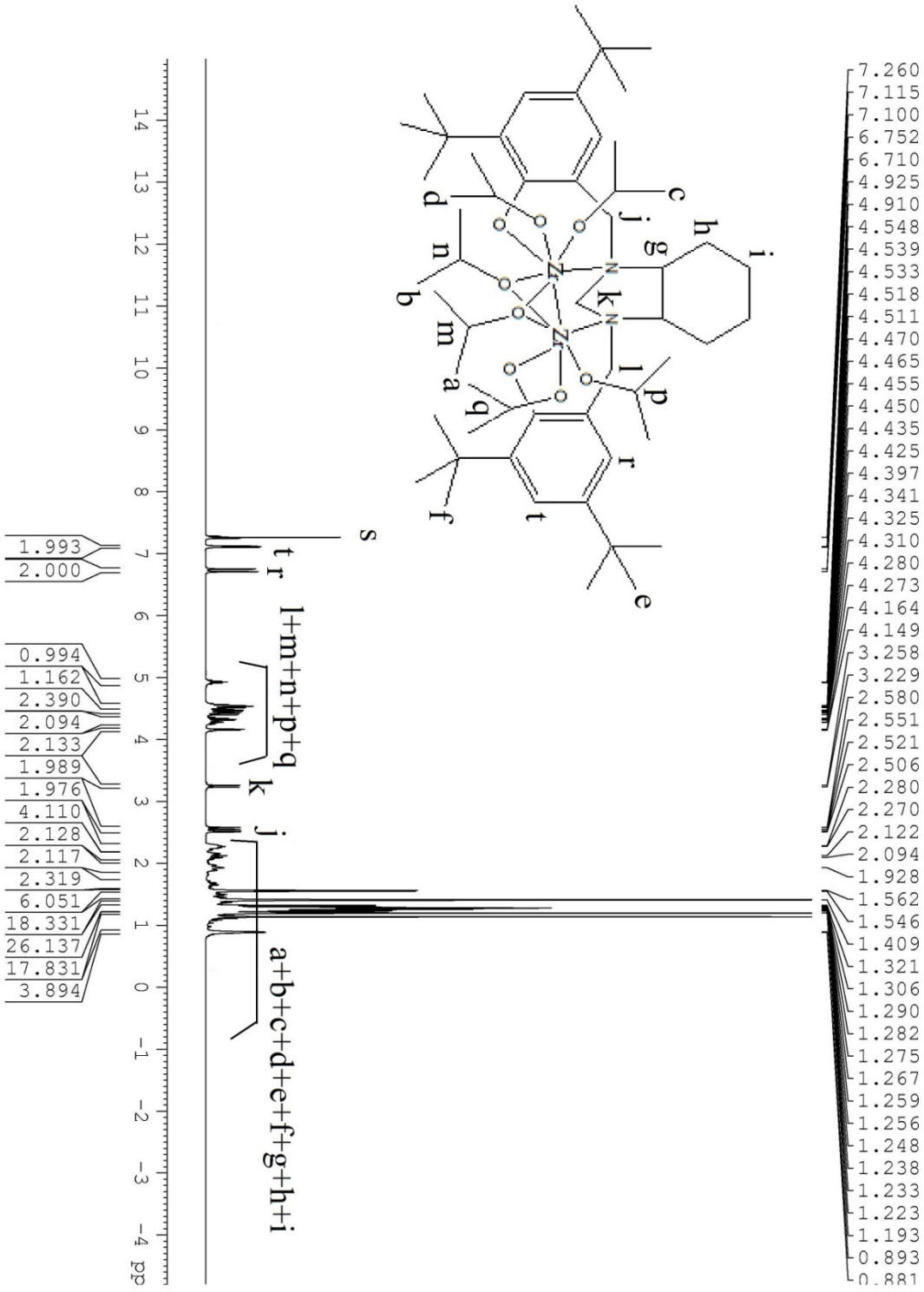

Fig. S7 ^{1}H NMR (400 MHz, $CDCl_3$) of Compound **3**

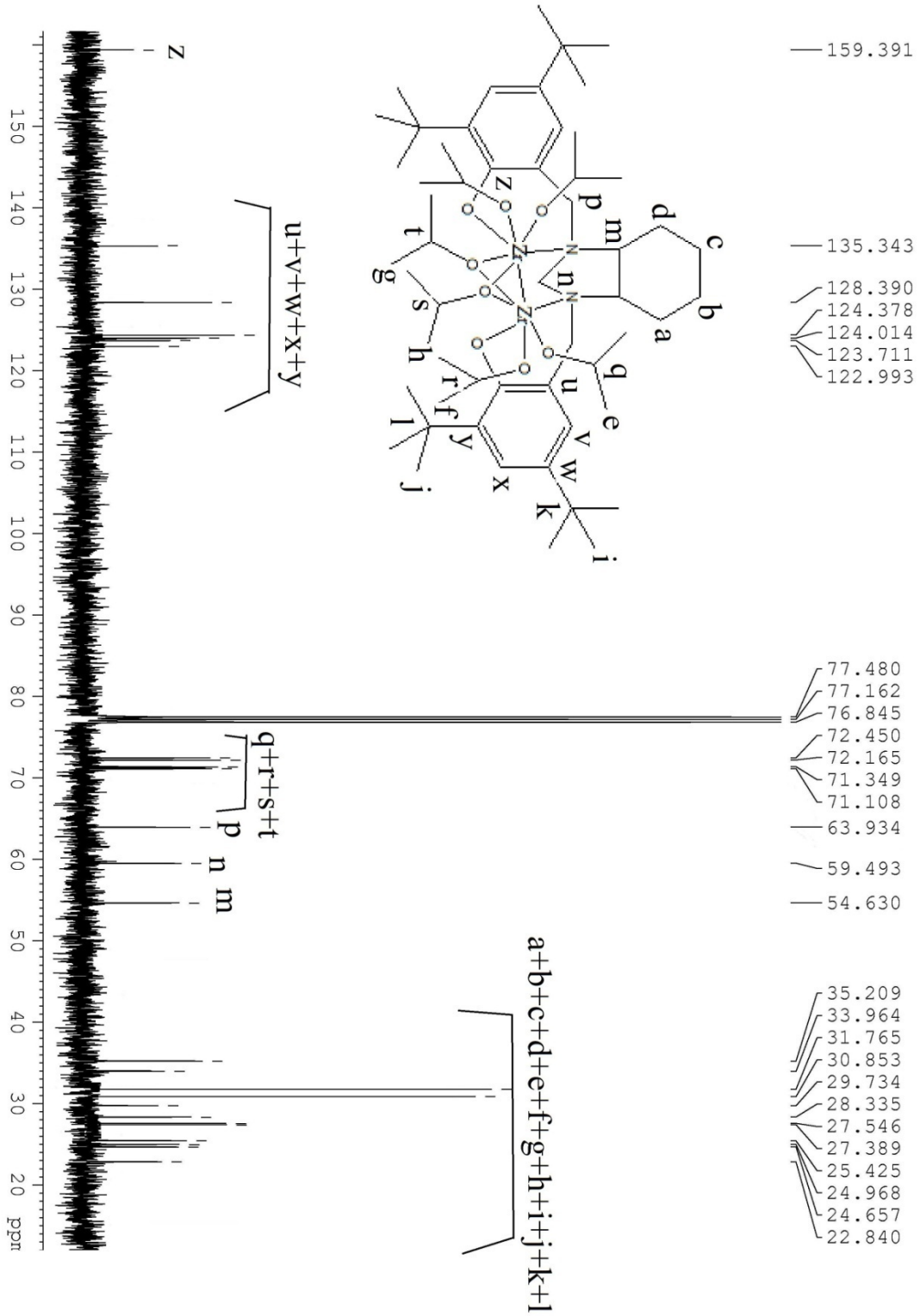

Fig. S8 ^{13}C NMR (100 MHz, $CDCl_3$) of Compound **3**

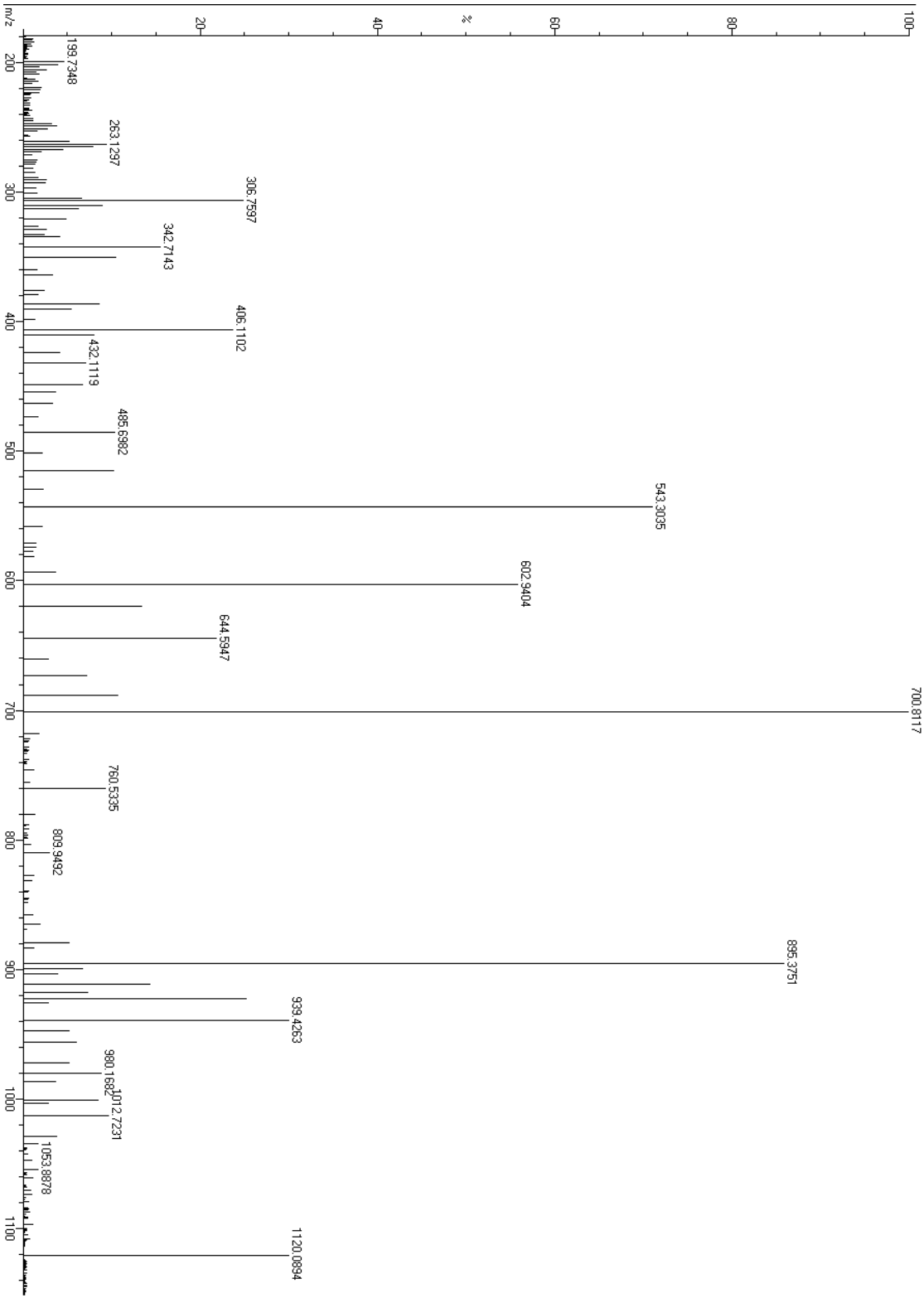

Fig. S9 ESI-Mass Spectrum of Compound **3**

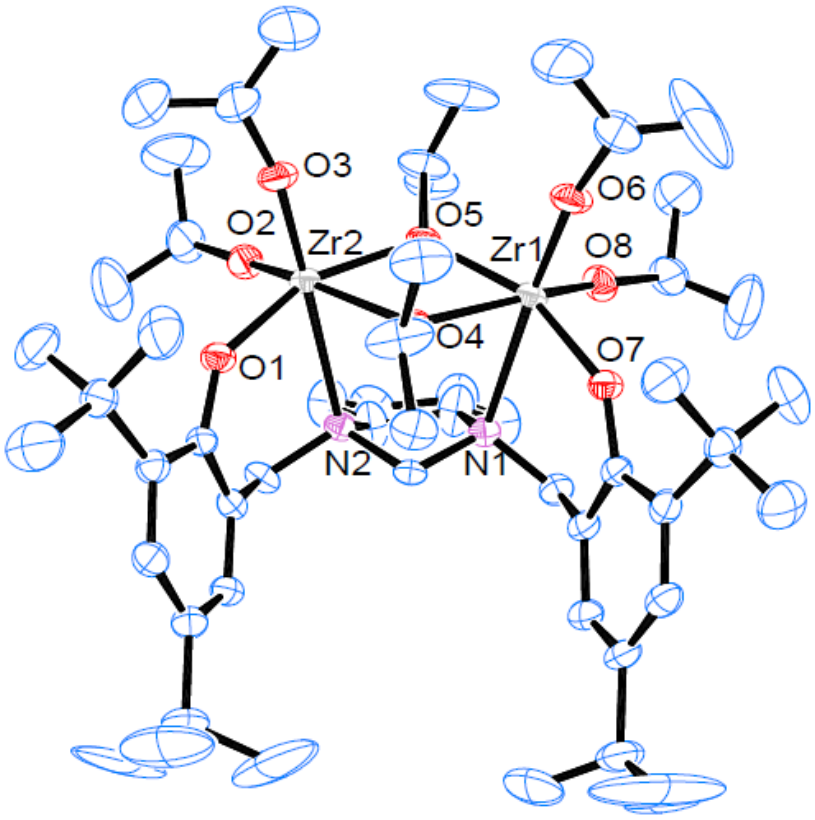

Fig. S10 Molecular structure of **3**; thermal ellipsoids were drawn at 30 % probability level. Selected bond lengths (Å) and bond angles (°): Zr(2)-O(1) 2.015(2), O(2)-Zr(2) 1.937(3), O(5)–Zr(2) 2.173(2), O(5)–Zr(1) 2.185(2), O(8)-Zr(1) 1.941(3), N(1)-Zr(1) 2.573(3), O(8)-Zr(1)-O(7) 97.28(11), O(3)-Zr(2)-O(1) 96.72(11)), O(8)-Zr(1)-N(1) 83.81(10), O(2)-Zr(2)-Zr(1) 97.95(11), O(8)-Zr(1)-Zr(2) 124.27(9), N(1)-Zr(1)-Zr(2) 76.55(6), O(6)-Zr(1)-O(7) 95.25(11), O(7)-Zr(1)-O(4) 94.72(9), Zr(2)-O(5)-Zr(1) 109.00(10).

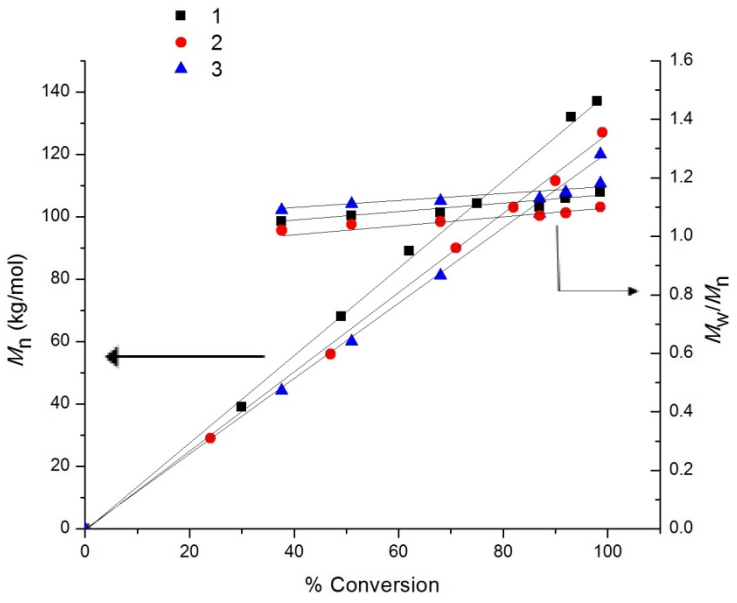

Fig. S11 Plot of M_n and M_w/M_n vs. % conversion for *rac*-LA polymerization at 140 °C using **1, 2** and **3**.

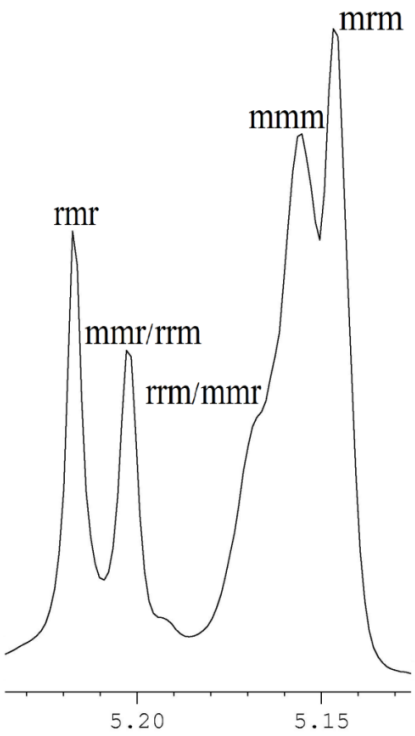

Fig. S12 Homonucler decoupled ^{1}H NMR spectra of *rac*-LA in 15:1 ratio using by **1** in $CDCl_3$.

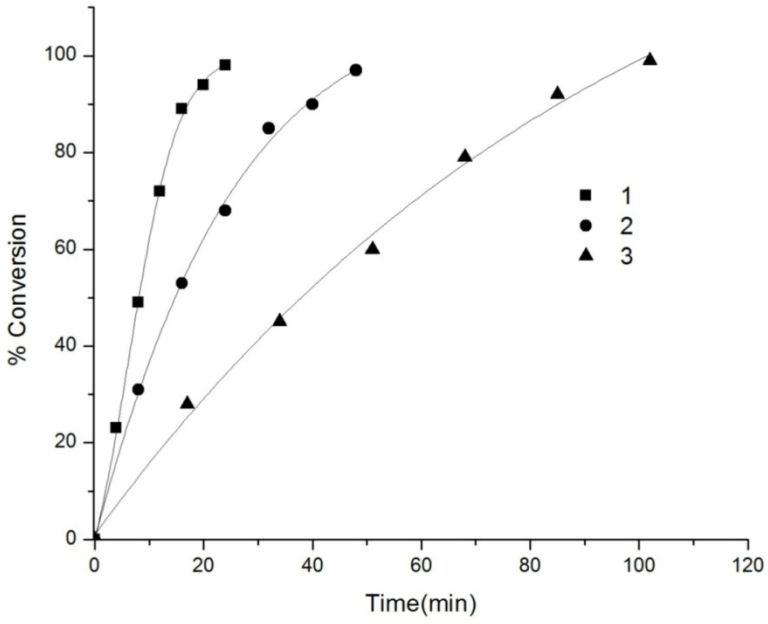

Fig. S13 *rac*-LA conversion vs. time plot using **1, 2** and **3**: $[rac\text{-LA}]_o/[Cat]_o = 600$ at 140 °C.

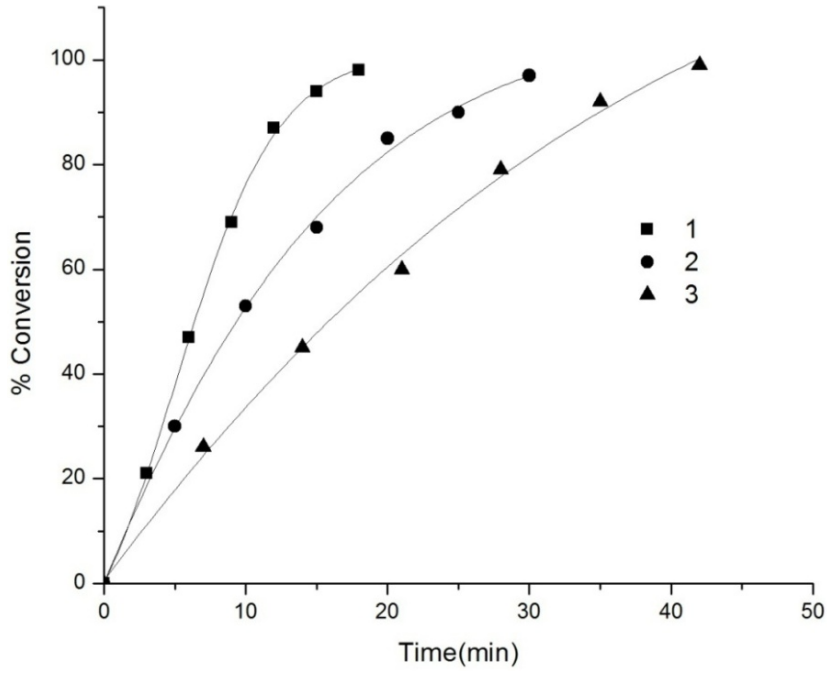

Fig. S14 ***ε*****-**CL conversion vs. time plot using **1, 2** and **3**: $[\varepsilon\text{-CL}]_o/[\text{Cat}]_o = 200$ at 80 °C.

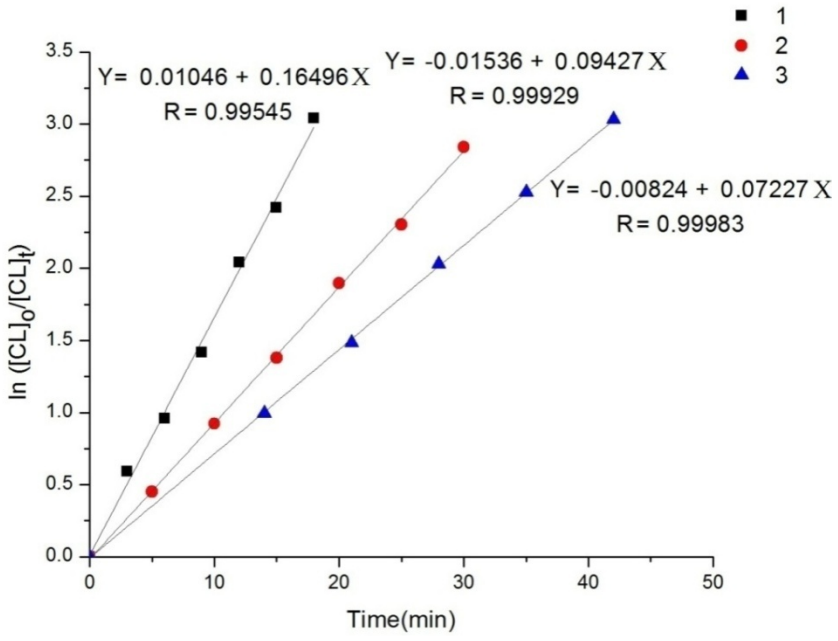

Fig. S15 Semi-logarithmic plots of *ε*-CL conversion in time initiated by **1, 2** and **3**: $[\varepsilon\text{-CL}]_o/[\text{Cat}]_o = 200$ at 80 ºC.

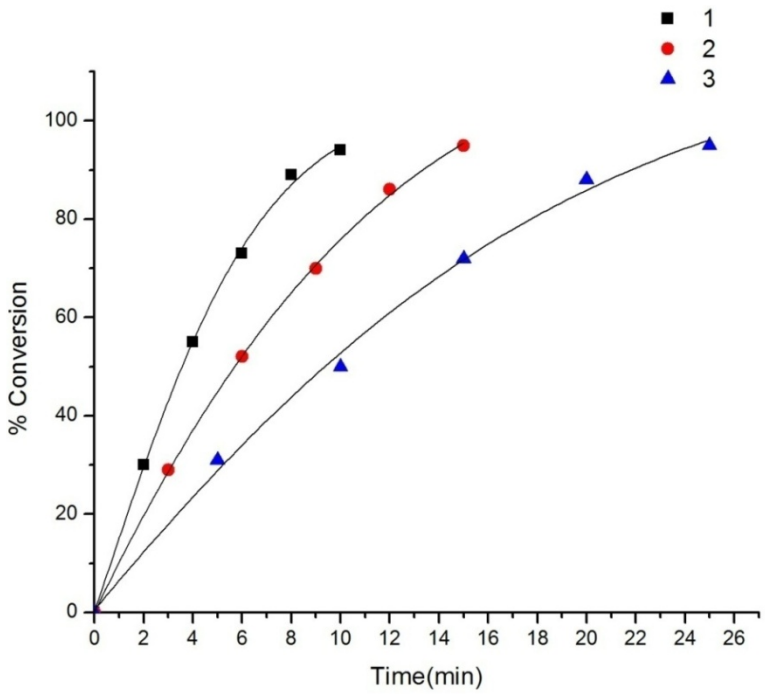

Fig. S16 *rac*-LA conversion vs. time plot using **1, 2** and **3**: $[rac\text{-LA}]_o/[Cat]_o/[BnOH]$ = 200:1:5 at 140 °C.

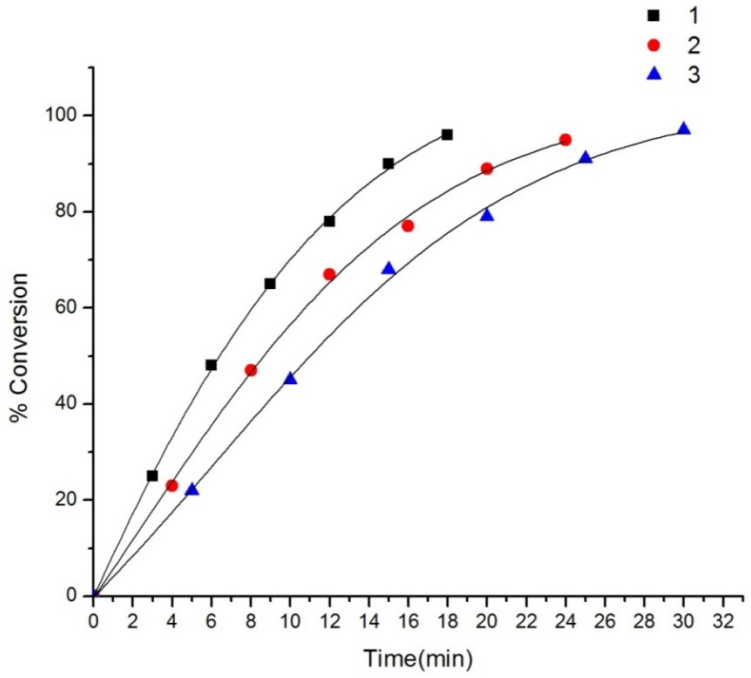

Fig. S17 *ε*-CL conversion vs. time plot using **1, 2** and **3**: $[\varepsilon\text{-CL}]_o/[Cat]_o/[BnOH]$ = 200:1:5 at 80 °C.

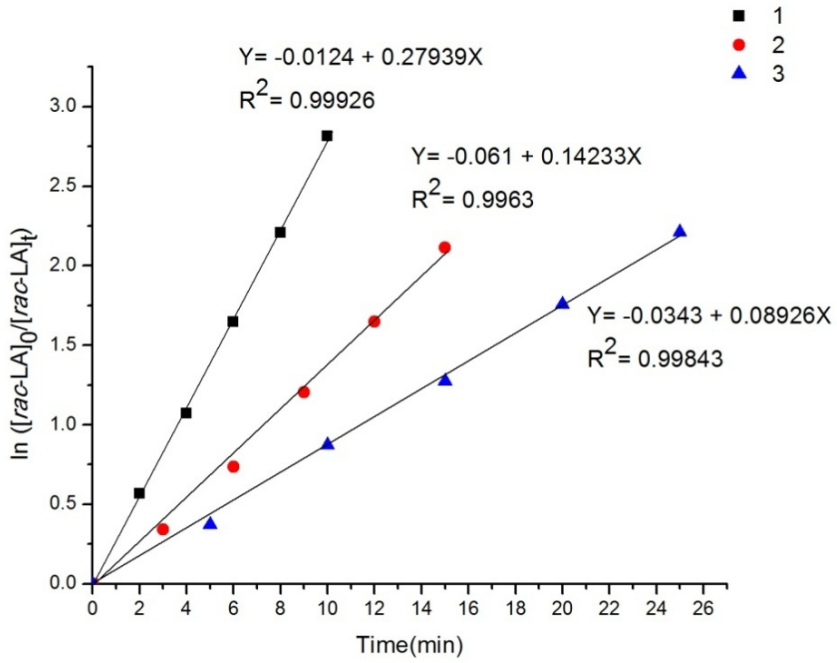

Fig. S18 Semi-logarithmic plots of *rac*-LA conversion in time initiated by **1, 2** and **3**: [*rac*-LA]$_o$/[Cat]$_o$/[BnOH] = 200:1:5 at 140 ºC.

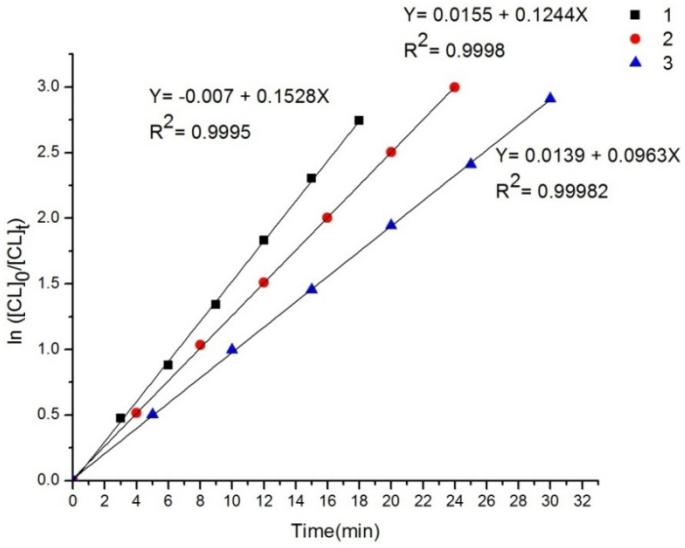

Fig. S19 Semi-logarithmic plots of **ε**-CL conversion in time initiated by **1, 2** and **3**: [**ε**-CL]$_o$/[Cat]$_o$/[BnOH] = 200:1:5 at 80 ºC.

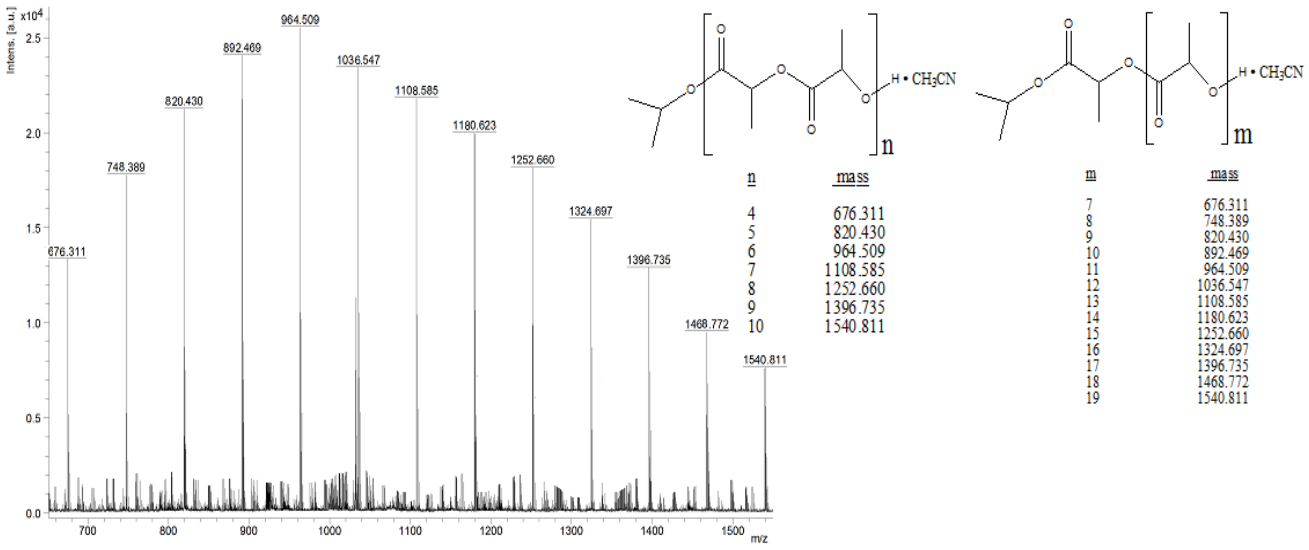

Fig. S20 MALDI-TOF of the crude product obtained from a reaction between *rac*-LA and 1 in 15:1 ratio. For n = 4, peak at 676.311 is observed [144.14* 4 + 59 (isopropoxide end group) + 41 (CH_3CN adduct)].

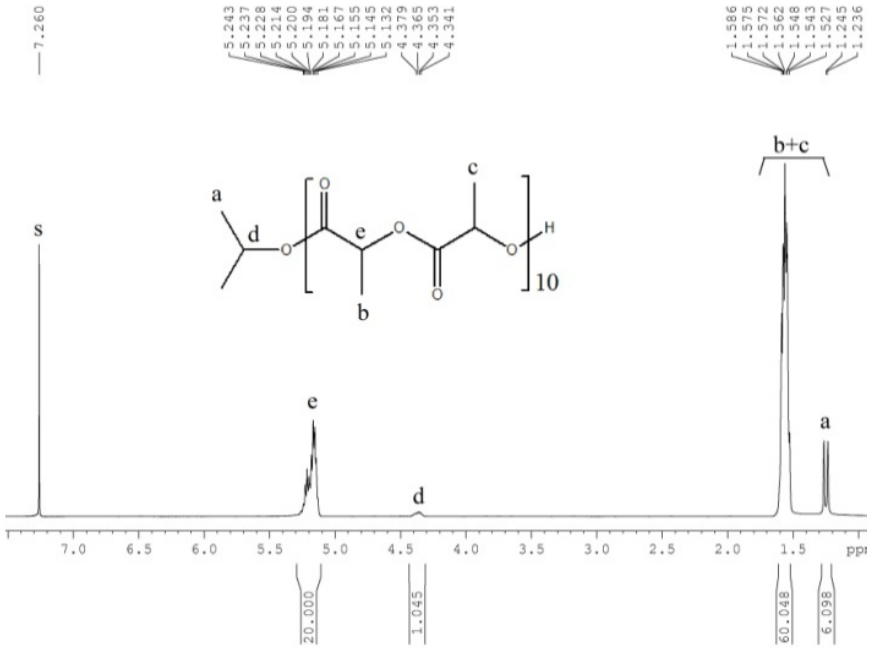

Fig. S21 ^{1}H NMR spectrum of the crude product obtained from a reaction between *rac*-LA and 1 in 15:1 ratio.

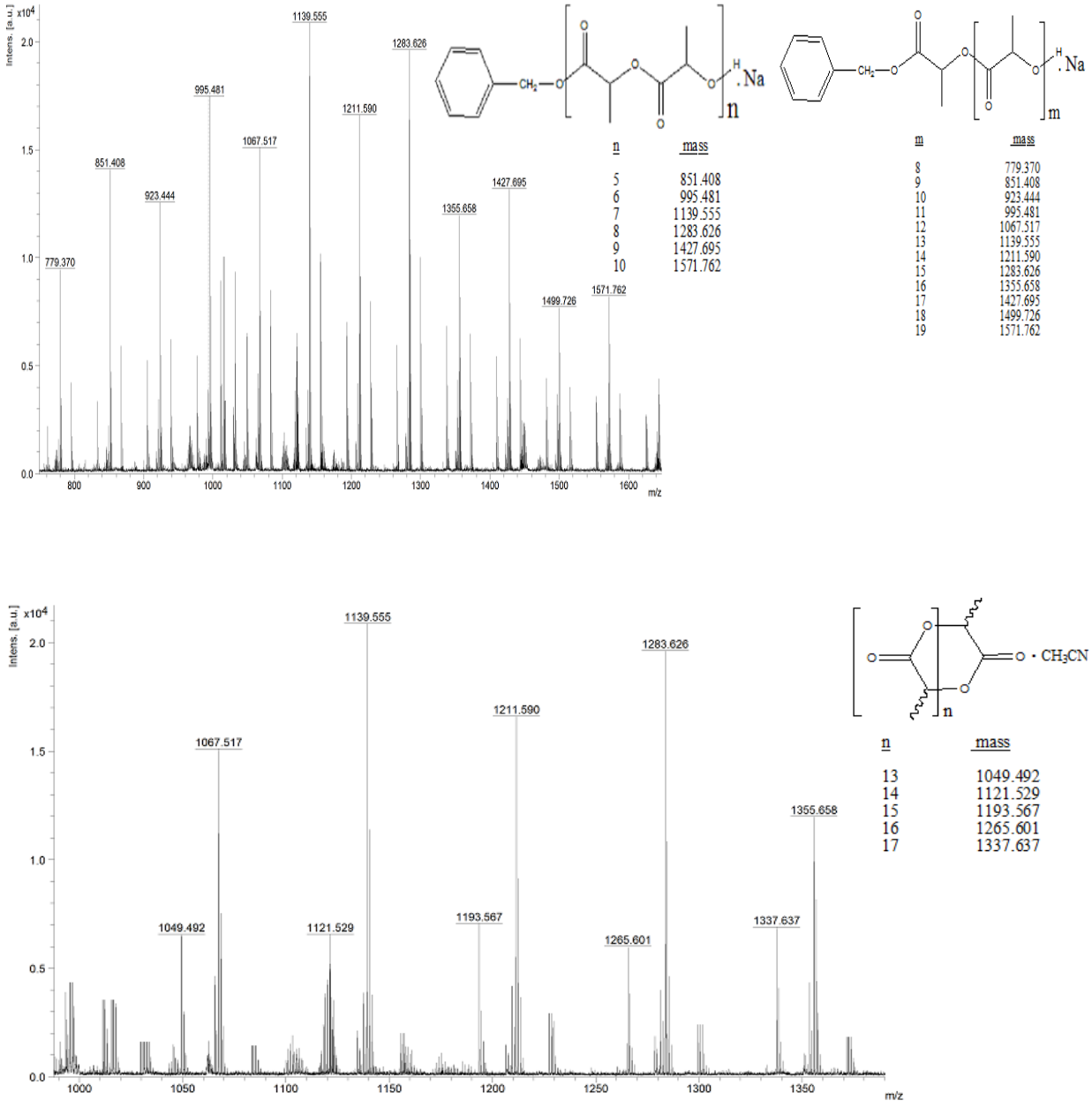

Fig. S22 MALDI-TOF of the crude product obtained from a reaction between *rac*-LA and 1 in the presence of BnOH in ratio 15:1:2. For n = 13, peak at 1049.492 is observed [72*13 + 72 + 41 (CH_3CN adduct)].

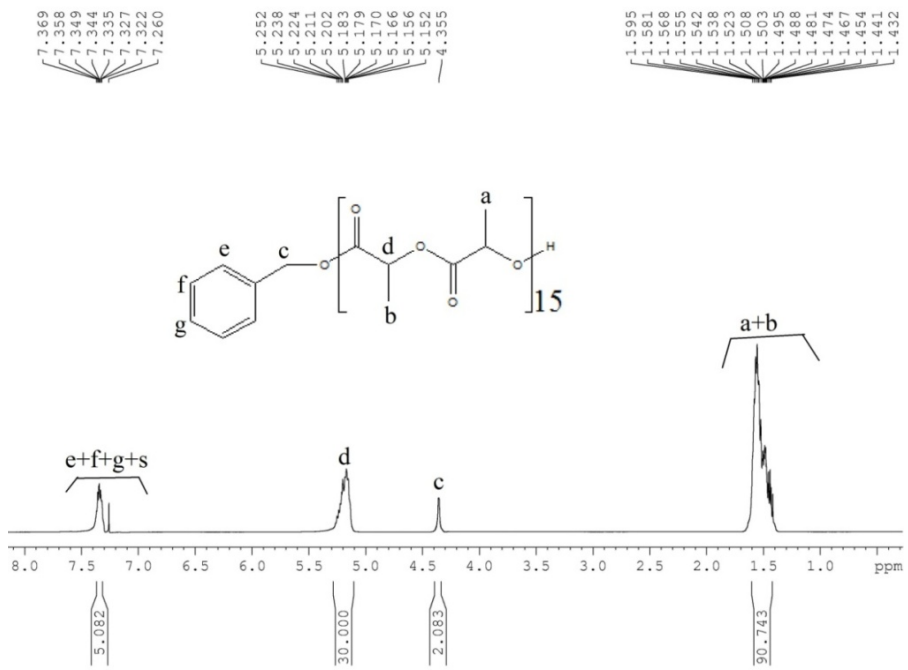

Fig. S23 [1]H NMR spectrum of the crude product obtained from a reaction between *rac*-LA and 1 in the presence of BnOH in ratio 15:1:2.

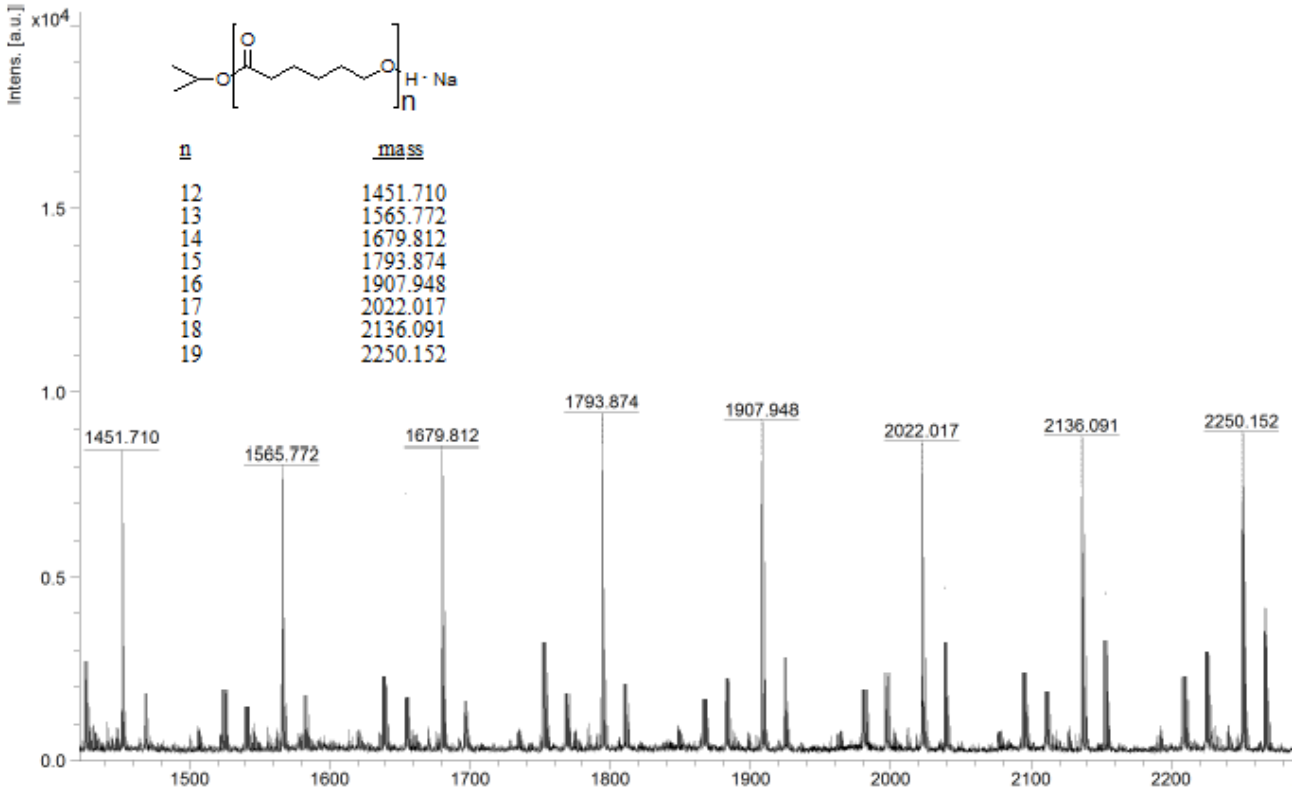

Fig. S24 MALDI-TOF of the crude product obtained from a reaction between **ε**-CL and **1** in 15:1 ratio.

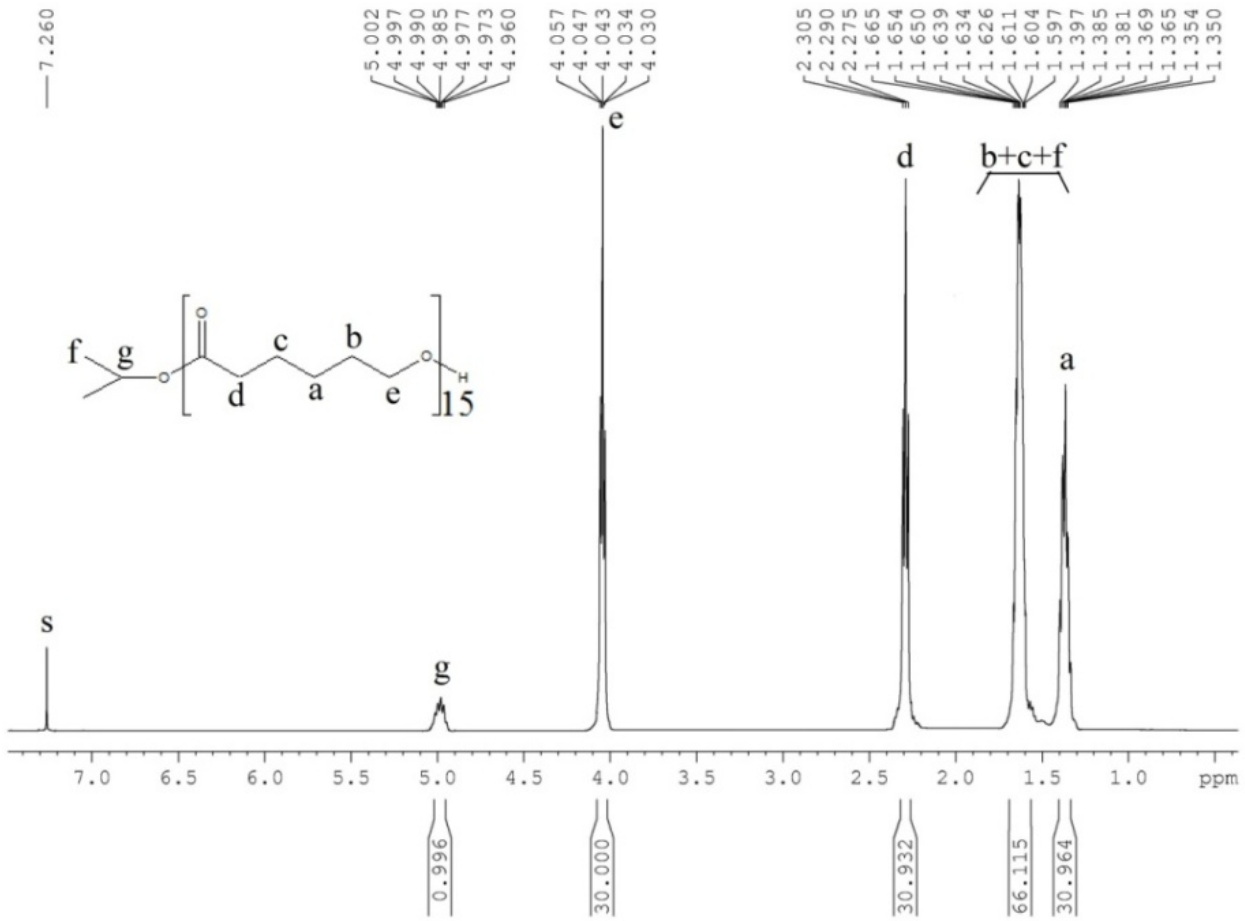

Fig. S25 ^{1}H NMR spectrum of the crude product obtained from a reaction between ***ε*-**CL and **1** in 15:1 ratio.

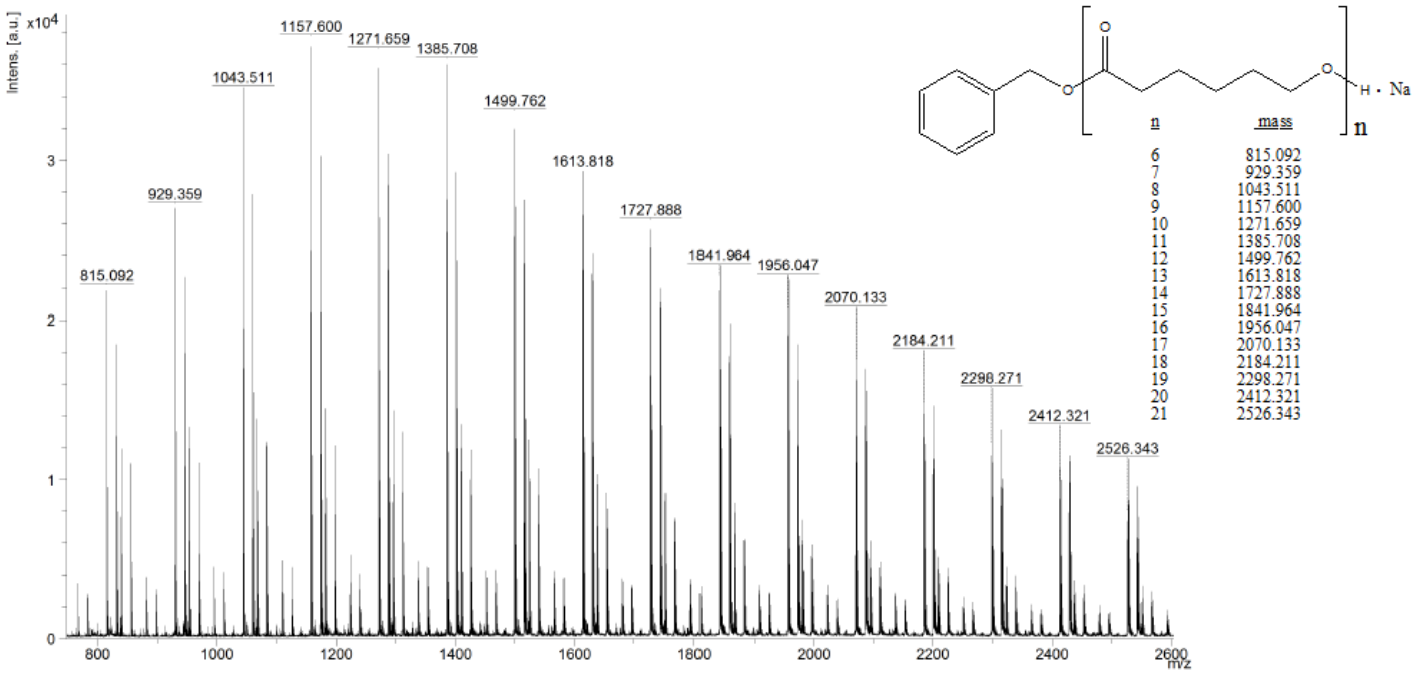

Fig. S26 MALDI-TOF of the crude product obtained from a reaction between ***ε***-CL and **1** in the presence of BnOH in ratio 15:1:2.

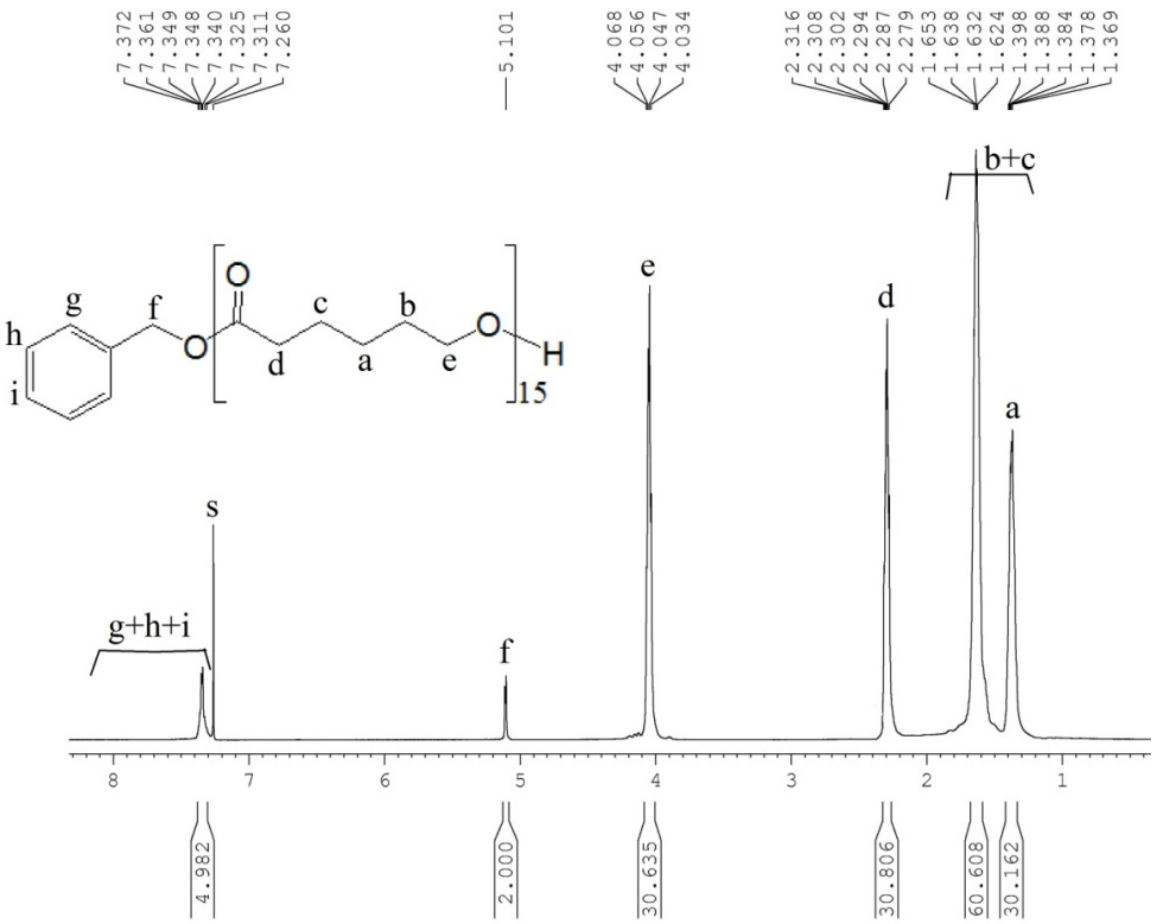

Fig. S27 ^{1}H NMR spectrum of the crude product obtained from a reaction between ***ε***-CL and **1** in the presence of BnOH in ratio 15:1:2.

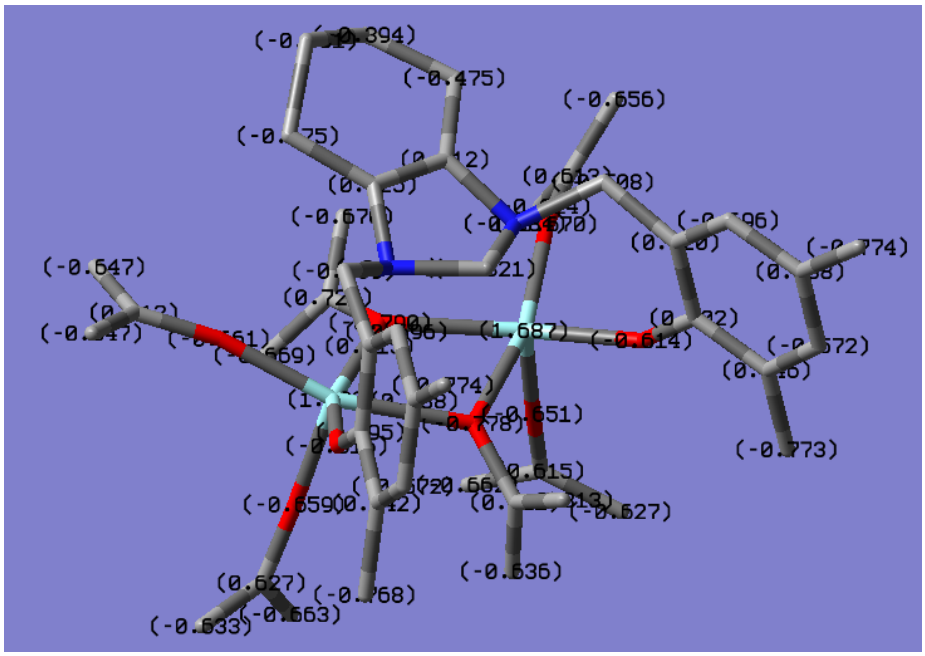

Complex **1**

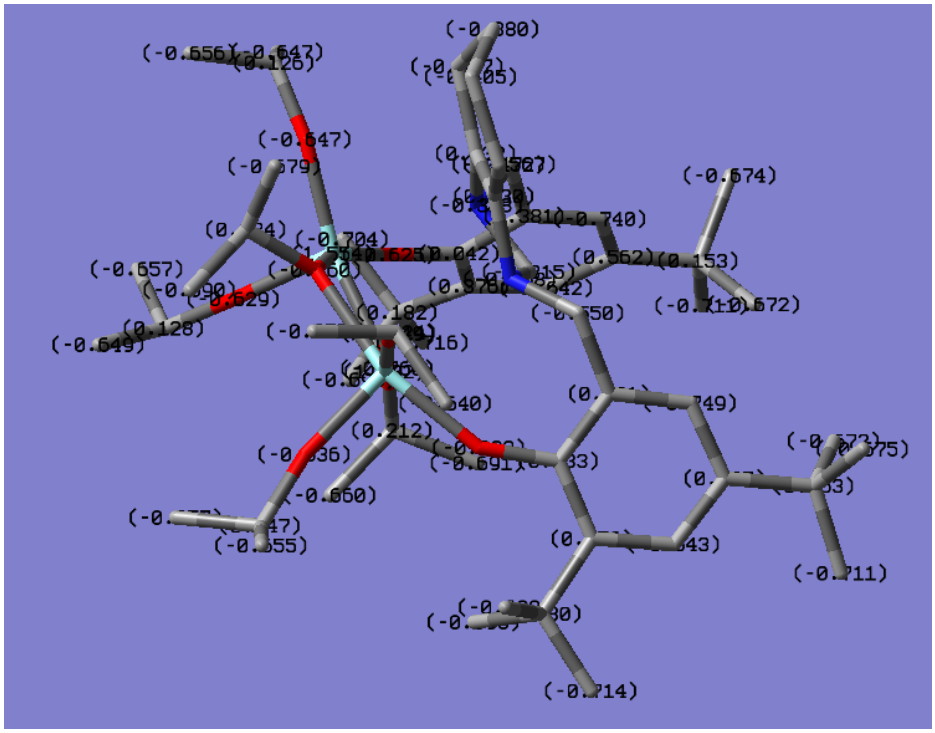

Complex **3**

Fig. S28 Mulliken partial charges of complexes **1** and **3**.

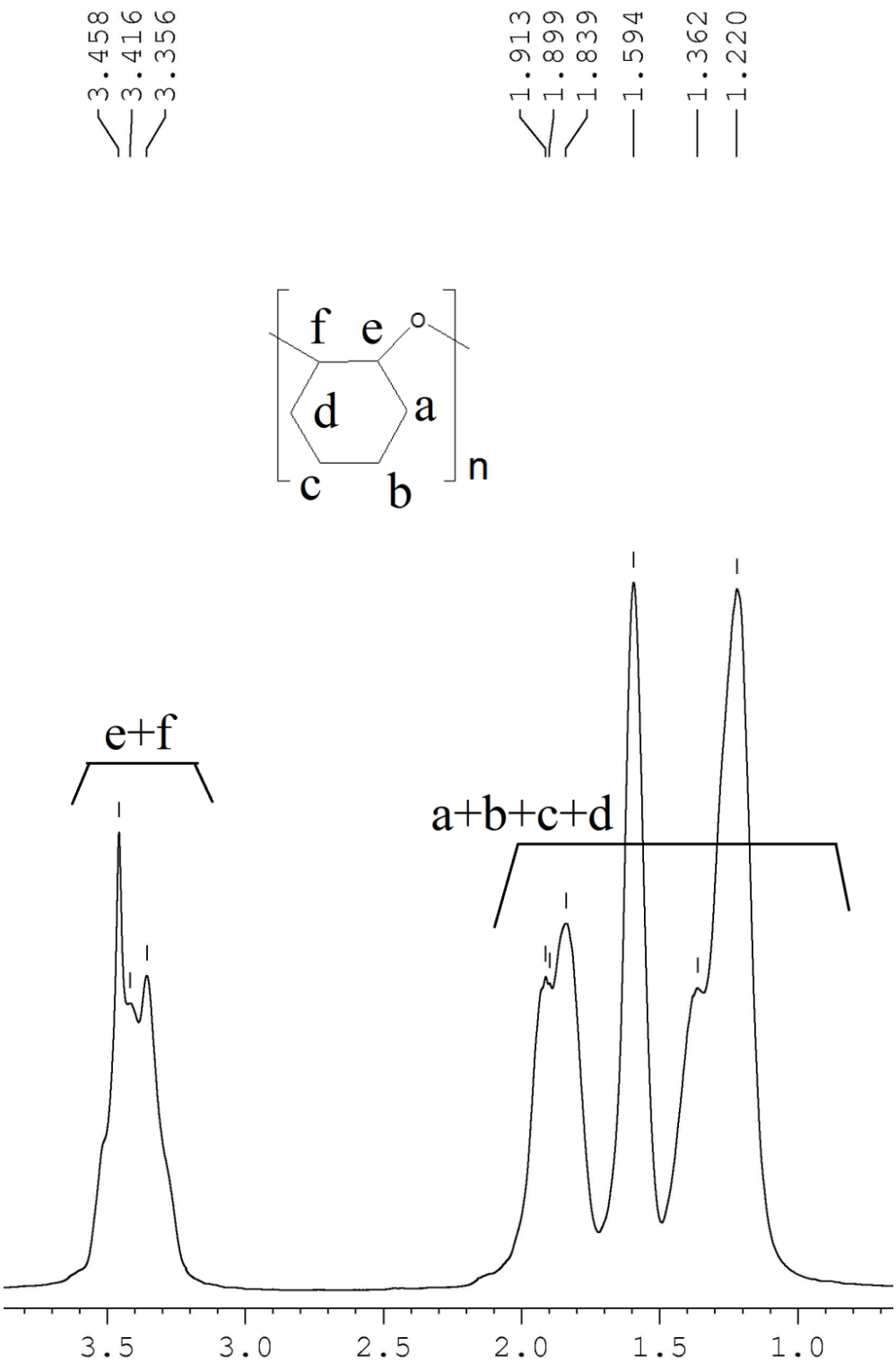

Fig. S29 ^{1}H NMR (500 MHz, $CDCl_3$) of the crude product obtained from a reaction between CHO and **1** in 1000:1 ratio at 80 °C.

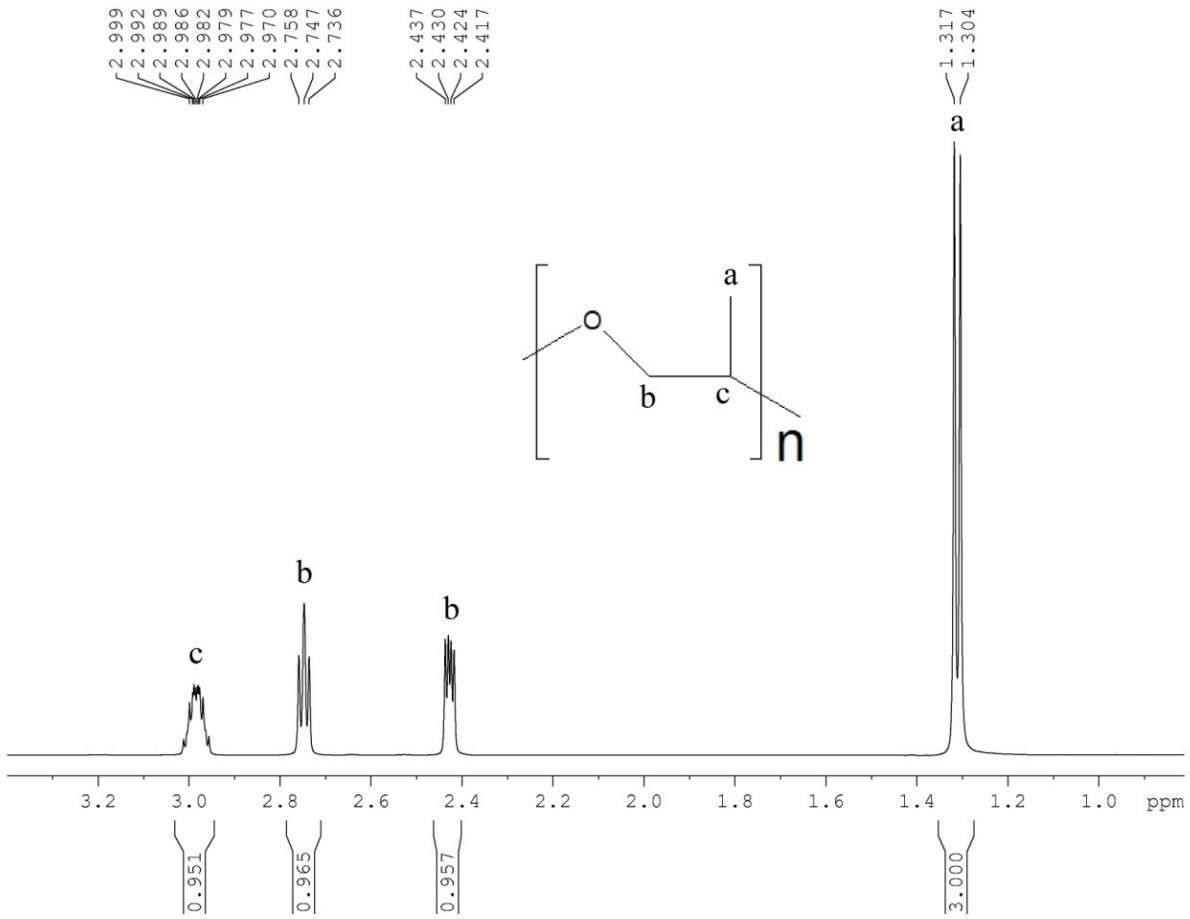

Fig. S30 ^{1}H NMR (500 MHz, $CDCl_3$) of the crude product obtained from a reaction between PO and **1** in 1000:1 ratio at 30 °C.

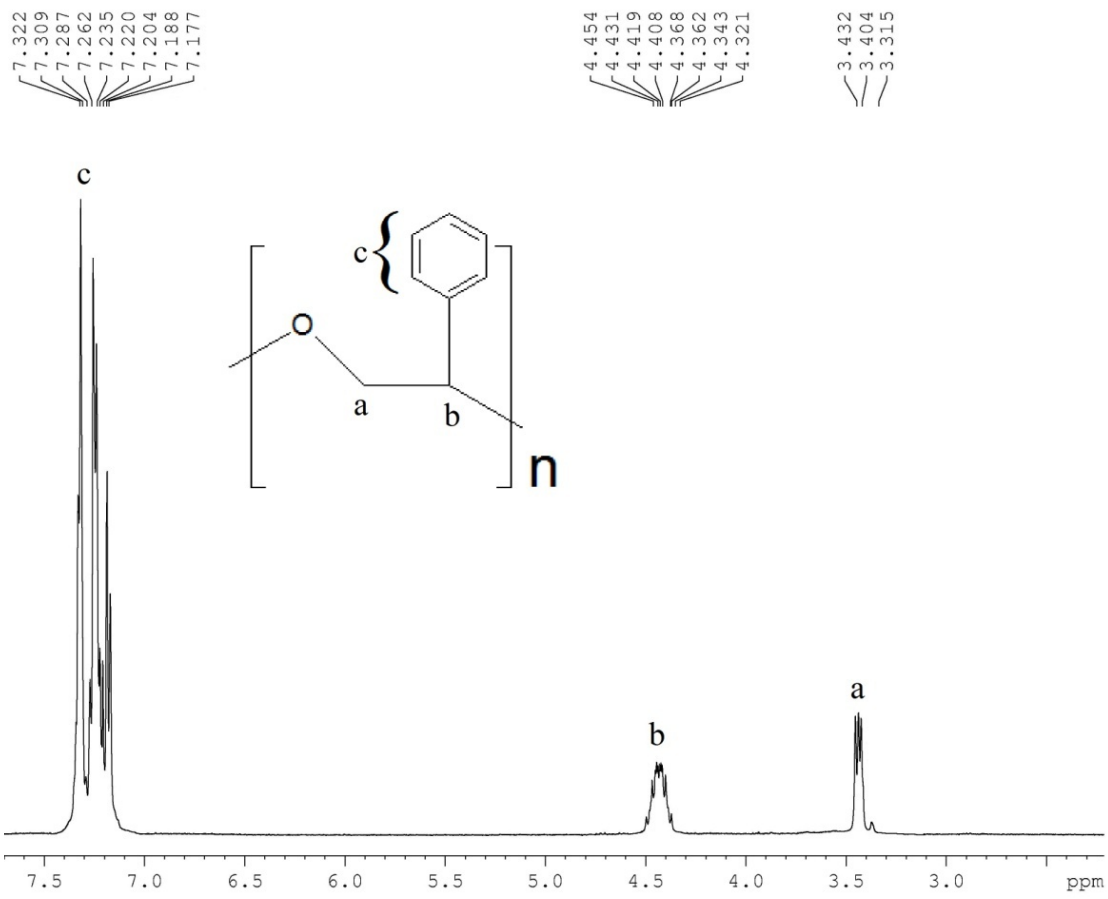

Fig. S31 ^{1}H NMR (500 MHz, $CDCl_3$) of the crude product obtained from a reaction between SO and **1** in 1000:1 ratio at 120 °C.

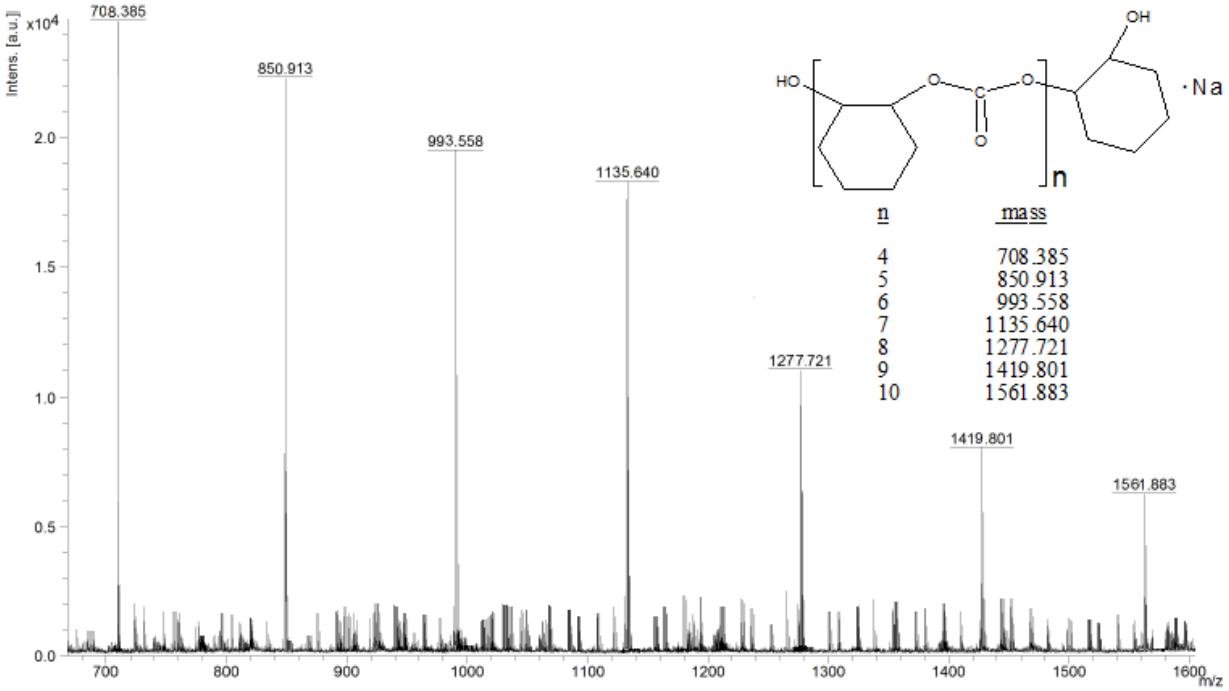

Fig. S32 MALDI-TOF mass spectrum of PCHC sample produced by **1** at 50 °C and 35 bar CO_2 pressure from CHO and CO_2 using TBAB as cocatalyst.

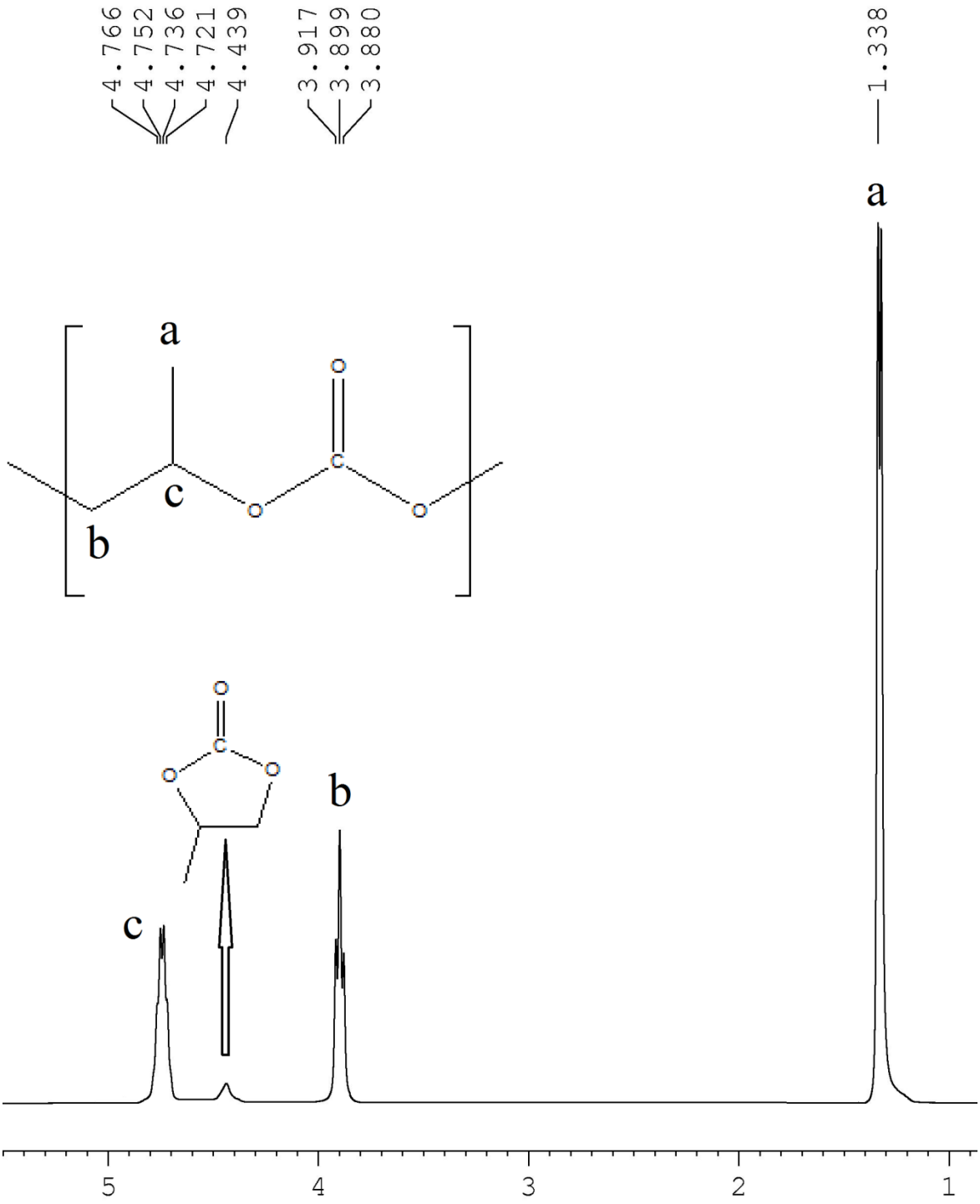

Fig. S33 ^{1}H NMR (500 MHz, $CDCl_3$) spectrum of a representative sample of poly(propylene carbonate).

Fig. S34 ^{13}C NMR (125 MHz, $CDCl_3$) spectrum of a representative sample of poly(propylene carbonate).

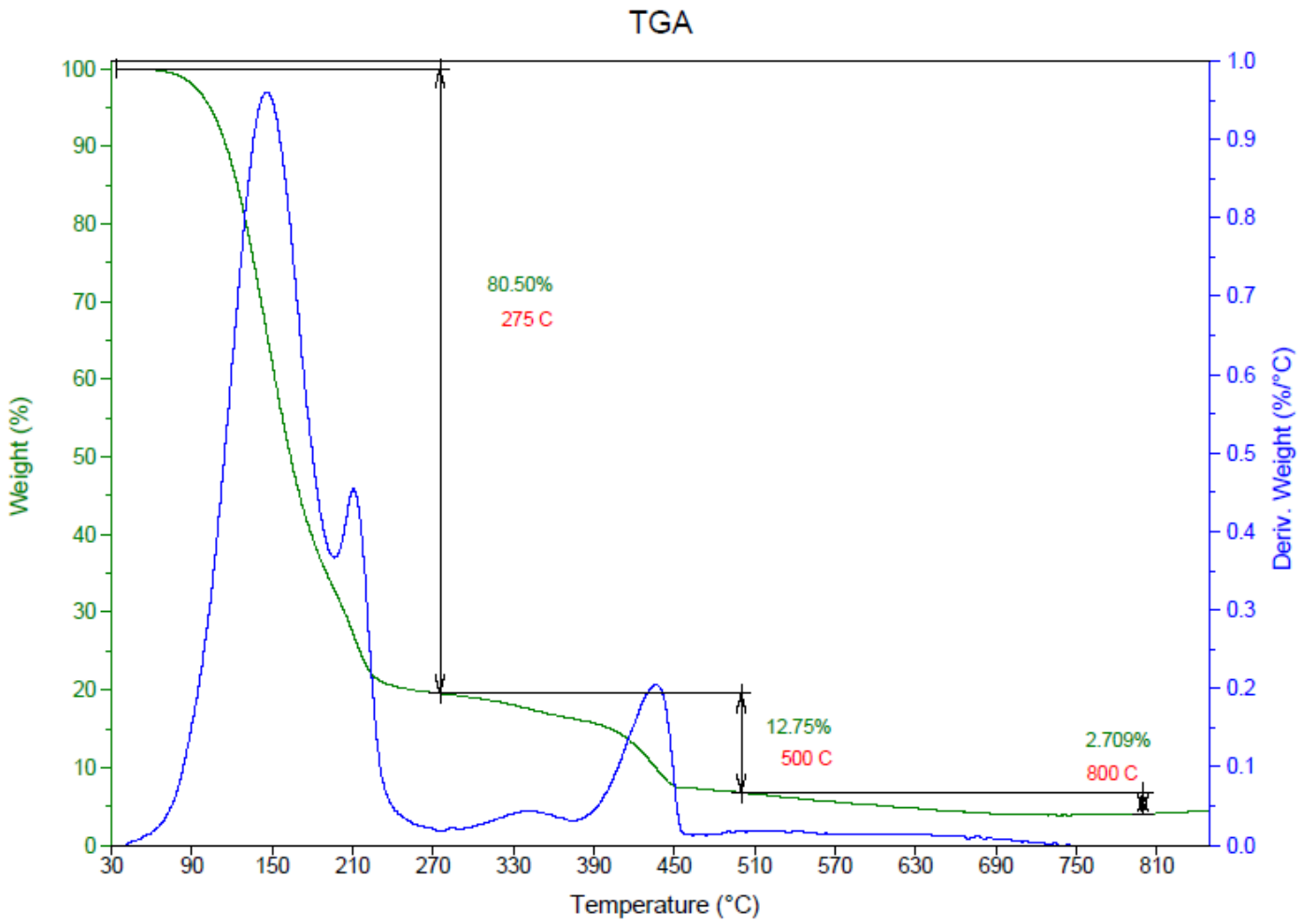

Fig. S35 Representative TGA trace and derivative plot of PCHC produced by **1** (Table 4, entry 1).

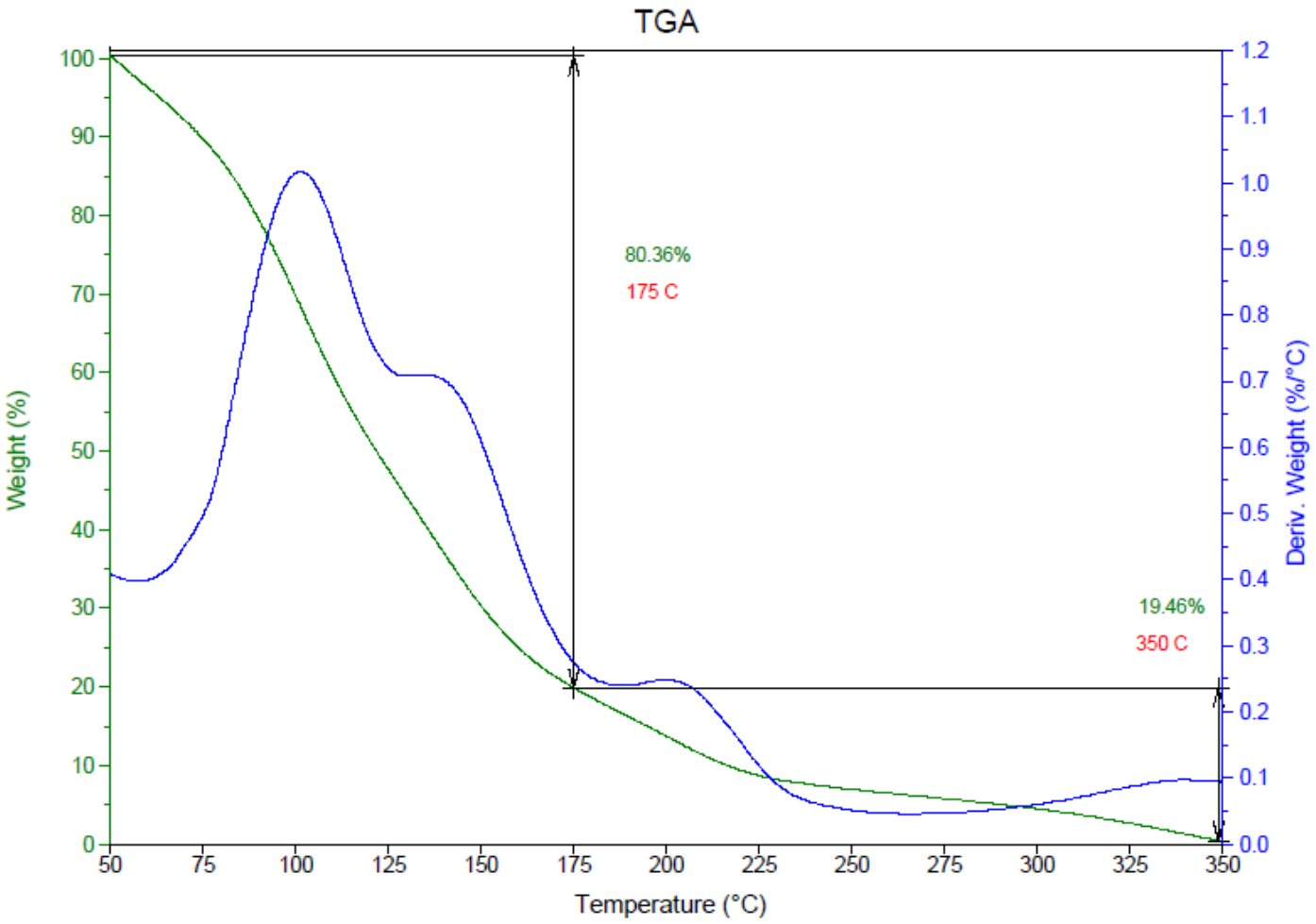

Fig. S36 Representative TGA trace and derivative plot of PPC produced by **1** (Table 4, entry 4).

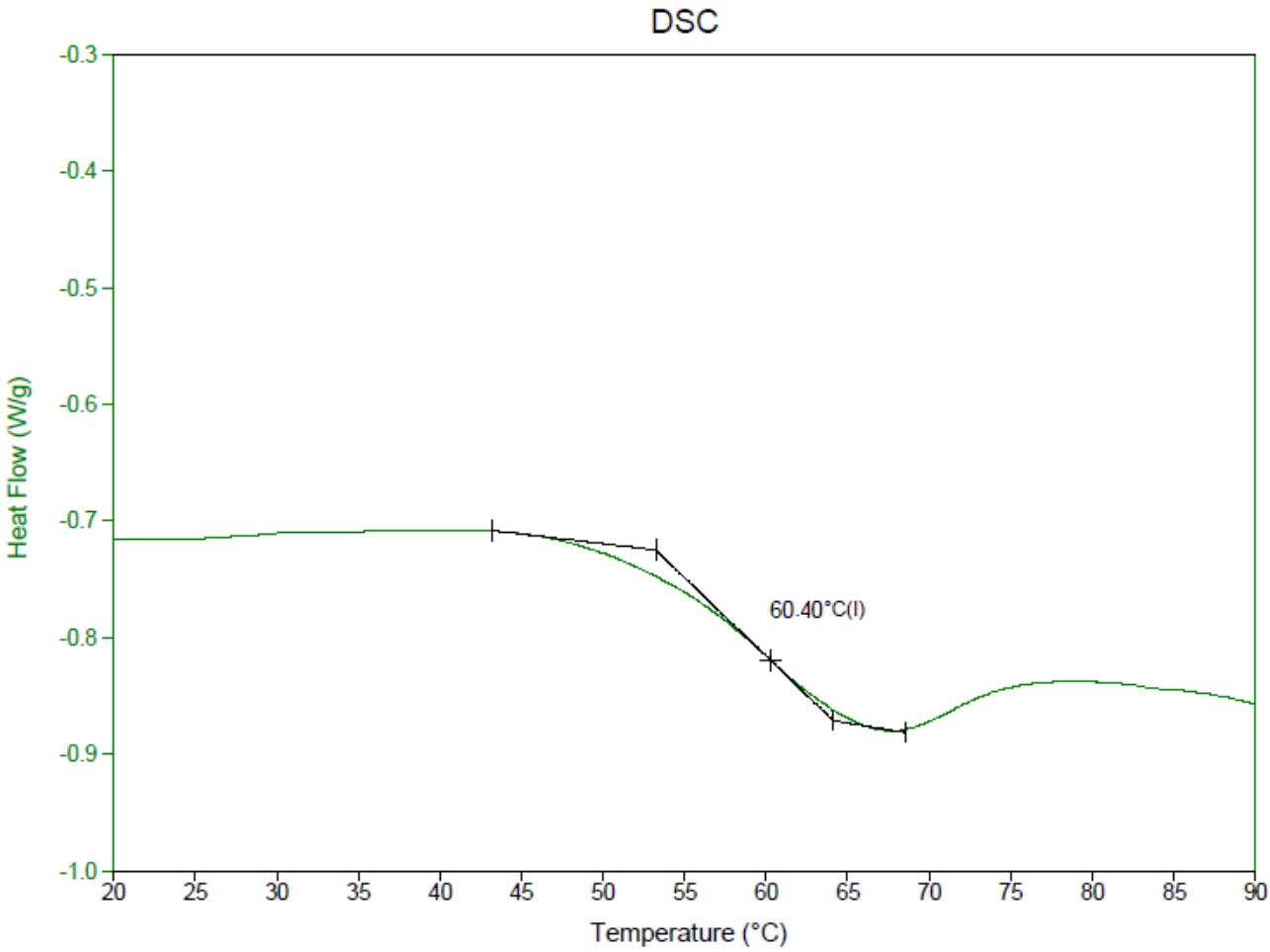

Fig. S37 Representative DSC trace of PCHC produced by **1**, 2nd heat cycle (Table 4, entry 1).

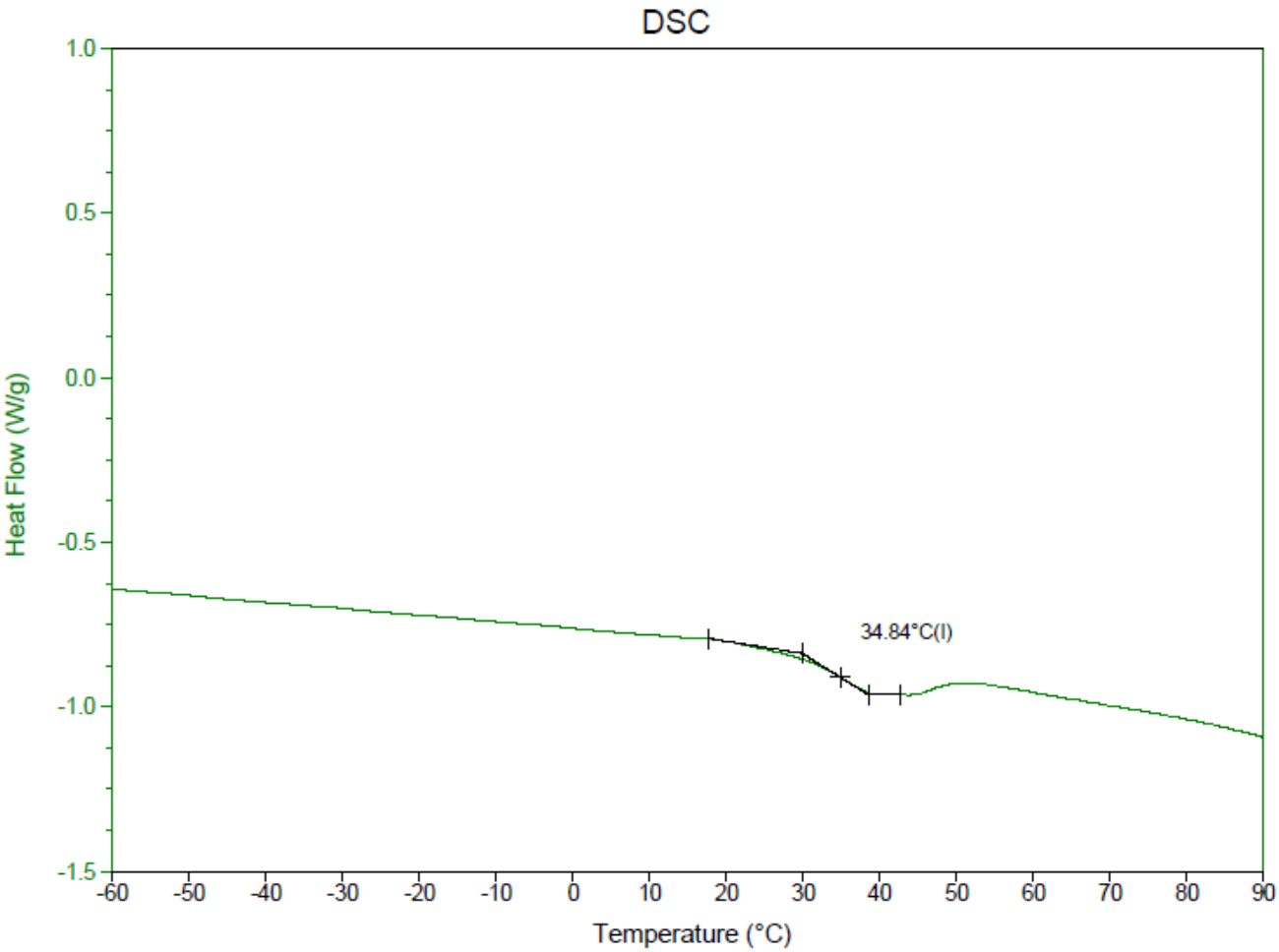

Fig. S38 Representative DSC trace of PPC produced by **1**, 2nd heat cycle (Table 4, entry 4).

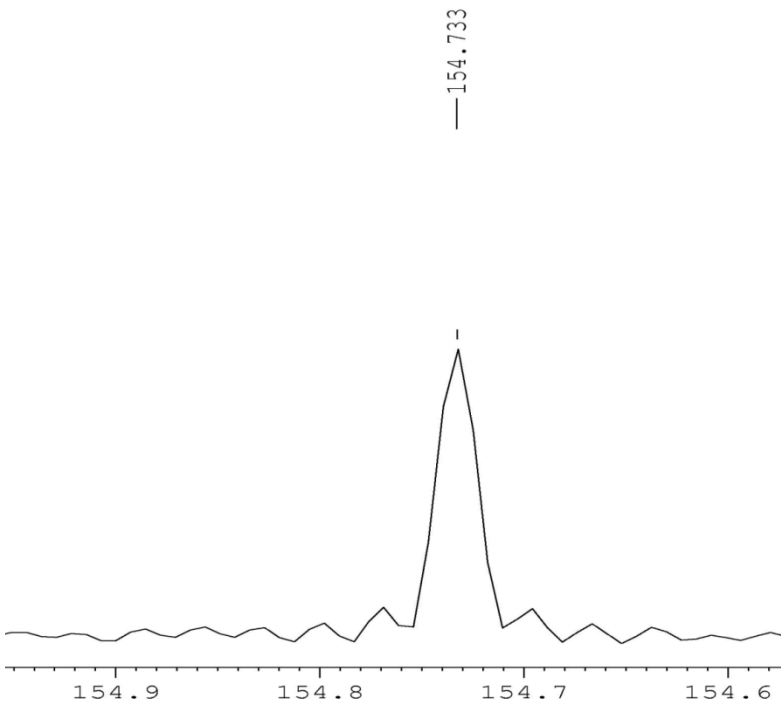

Fig. S39 Carbonyl region of the ^{13}C-NMR spectrum of styrene carbonate (SC) synthesized from the coupling of styrene oxide (SO) and CO_2.

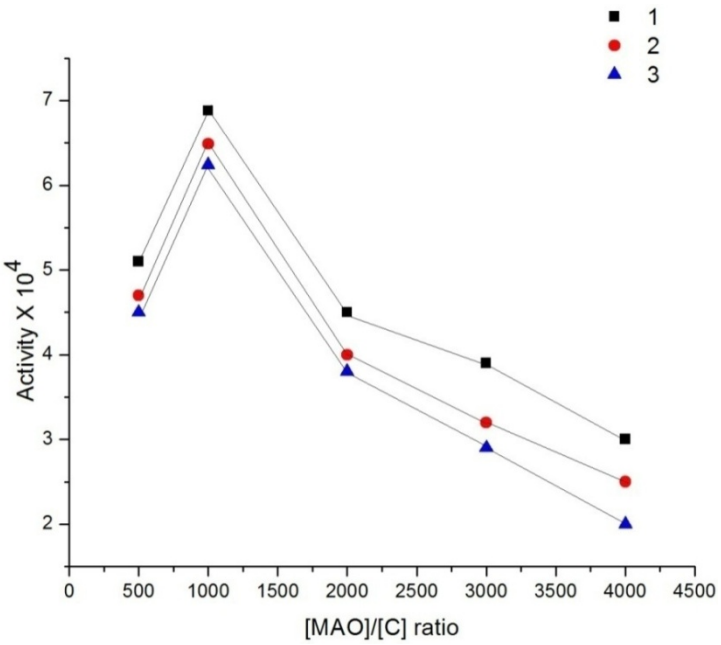

Fig. S40 Plot of activity *vs*. [MAO]/[cat] ratio for **1**, **2** and **3** for ethylene polymerization.

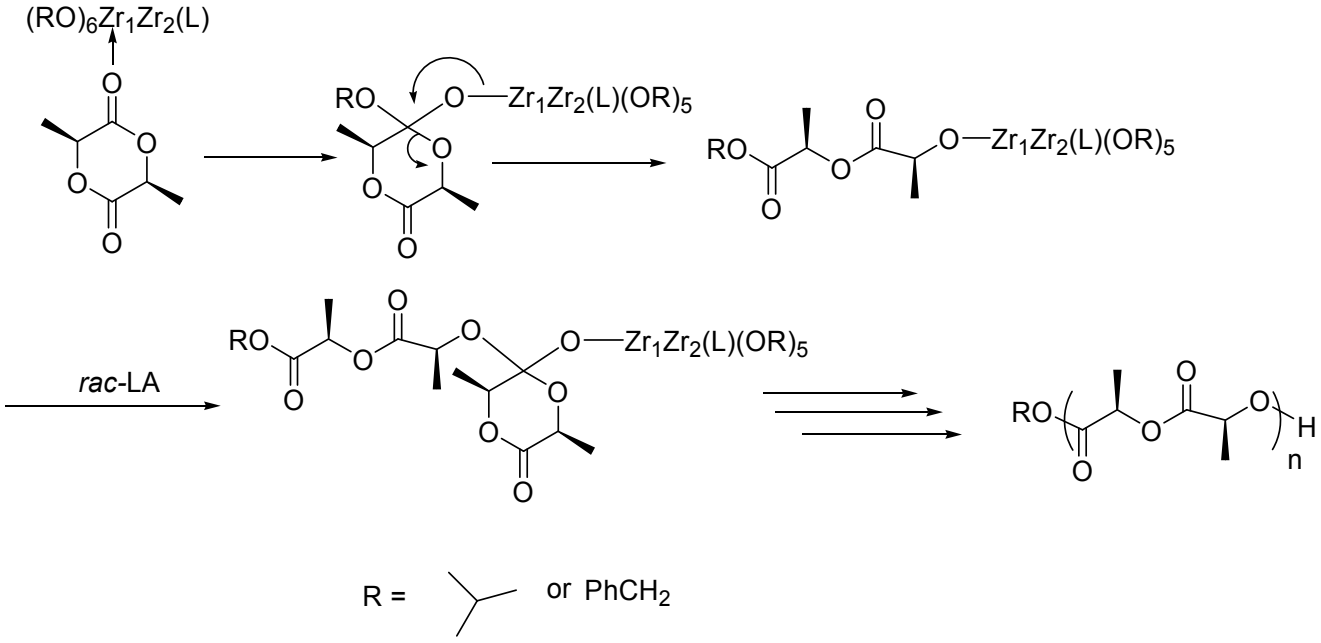

Scheme S1 Polymerization proceeds through the coordination-insertion mechanism for *rac*-LA.

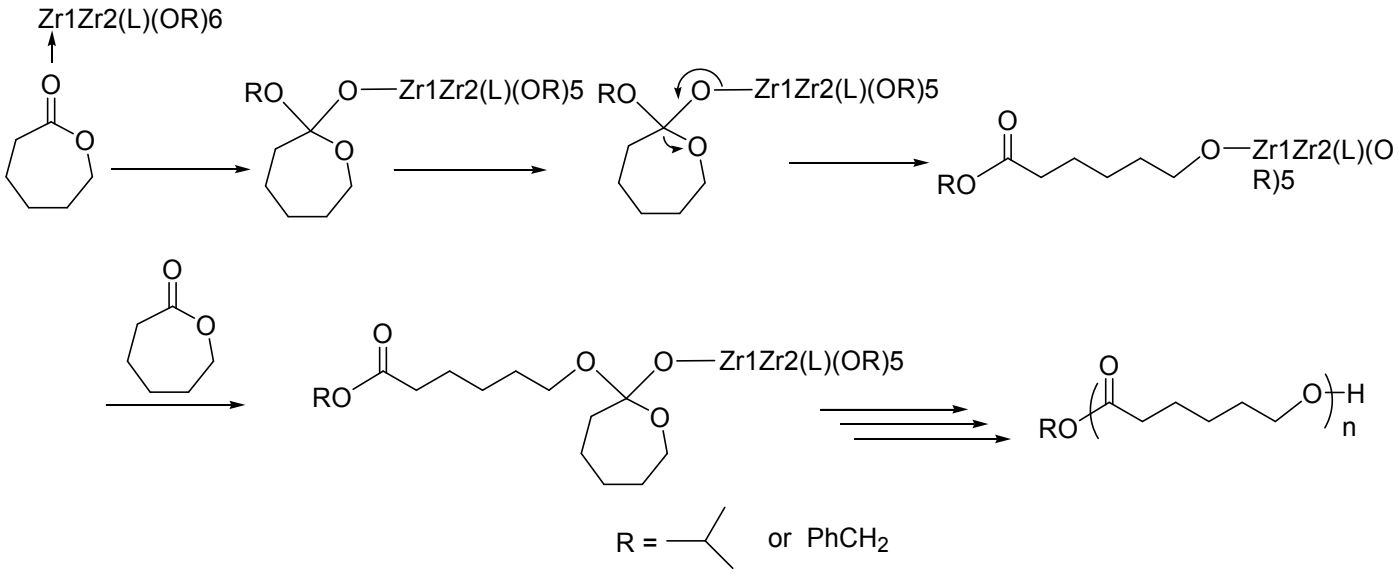

Scheme S2 Polymerization proceeds through the coordination-insertion mechanism for **ε-**CL.

Table S1 Crystal data for the structures of **1, 2** and **3**

Compound	**1**	**2**	**3**
Empirical formula	$C_{43}H_{71}N_2O_8Zr_2$	$C_{49}H_{86}N_2O_8Zr_2$	$C_{59}H_{96}N_2O_8Zr_2$
Formula weight	926.46	1013.64	1143.82
Crystal system	Monoclinic	Monoclinic	Triclinic
Space group	*P*2(1)/*n*	*P*21/*c*	*P*1
Temp/K	298(2)	296(2)	298(2)
Wavelength (Å)	0.71073	0.71073	0.71073
a (Å)	11.9483(4)	16.8978(5)	11.1760(3)
b (Å)	21.6468(7)	13.4806(4)	11.3344(3)
c (Å)	19.0429(5)	24.3958(7)	26.2444(8)
α (°)	90	90	94.360(2)
β (°)	101.575(2)	102.6790(10)	101.224(2)
γ (°)	90	90	100.485(2)
V (Å^3)	4825.1(3)	5421.7(3)	3184.95(15)
Z	4	4	2
D_{calc} (g/cm^3)	1.275	1.242	1.193
Reflns collected	29680	45770	38478
No. of indepreflns	8488	9539	11145
GOF	1.047	0.853	1.195
Final *R* indices($I>2\sigma(I)$)	$R_1 = 0.0409$, $wR_2 = 0.1007$	$R_1 = 0.0473$, $wR_2 = 0.1374$	$R_1 = 0.0472$, $wR_2 = 0.1464$
R indices (all data)	$R_1 = 0.0678$, $wR_2 = 0.1230$	$R_1 = 0.0615$, $wR_2 = 0.1613$	$R_1 = 0.0684$, $wR_2 = 0.1672$

$R_1 = \sum|F_0| - |F_c|/\sum|F_0|$, $wR_2 = [\sum (F_0^2 - F_c^2)^2/\sum w(F_0^2)^2]^{1/2}$

Table S2 Solution polymerization data for *rac*-LA and ***ε***-CL using **1–3** in the presence of benzyl alcohol in 200:1:5 (monomer: catalyst: benzyl alcohol) ratio.

Entry	Initiator	Monomer	T / °C	Yield (%)	[a]Time/ min	[b]TOF/min	[c]M_n^{obs}/ kgmol^{-1}	[d]M_n^{theo}/ kgmol^{-1}	M_w/M_n	[e]P_r
1	**1**	*rac*-LA	140	98	11	3.6	6.89	5.87	1.05	0.72
2	**2**	*rac*-LA	140	99	16	2.5	6.81	5.87	1.09	0.71
3	**3**	*rac*-LA	140	99	27	1.5	6.02	5.87	1.10	0.73
4	**1**	***ε***-CL	80	97	19	2.0	6.73	4.67	1.08	
5	**2**	***ε***-CL	80	98	25	1.6	5.55	4.67	1.13	
6	**3**	***ε***-CL	80	98	31	1.3	5.69	4.67	1.11	

[a]Time of polymerization measured by quenching the polymerization reaction when all monomer was found consumed. [b]Turnover frequency (TOF) = Number of moles of monomer consumed / (mole of catalyst × time of polymerization). [c]Measured by GPC at 27 °C in THF relative to polystyrene standards with Mark-Houwink corrections for M_n for ***ε***-CL and LA polymerization. [d]M_n (theoretical) at 100 % conversion = $[M]_o/[C]_o$ × mol wt (monomer) + mol wt (BnOH). [e]Calculated from homonuclear decoupled ^{1}H NMR spectrum.

Table S3 Computed Mulliken Net charges (Q/e) on various atoms of complexes **1** and **3**

Complex	Positions	Mulliken Charge (Q/e)
1	Ph-*O* (1)	–0.615
	Ph-*O* (2)	–0.614
	^{i}Pr-*O* (terminal 1)	–0.651
	^{i}Pr-*O* (terminal 2)	–0.659
	^{i}Pr-*O* (terminal 3)	–0.661
	^{i}Pr-*O* (terminal 4)	–0.670
	^{i}Pr-*O* (bridging 1)	–0.778
	^{i}Pr-*O* (bridging 2)	–0.790
3	Ph-*O* (1)	–0.625
	Ph-*O* (2)	–0.632
	^{i}Pr-*O* (terminal 1)	–0.629

3	^{i}Pr-*O* (terminal 2)	–0.636
	^{i}Pr-*O* (terminal 3)	–0.647
	^{i}Pr-*O* (terminal 4)	–0.649
	^{i}Pr-*O* (bridging 1)	–0.760
	^{i}Pr-*O* (bridging 2)	–0.760